

MIT Open Access Articles

Search for top squarks in final states with two top quarks and several light-flavor jets in proton-proton collisions at $\sqrt{s}=13$ TeV

The MIT Faculty has made this article openly available. **Please share** how this access benefits you. Your story matters.

Citation: Harris, Philip. 2021. "Search for top squarks in final states with two top quarks and several light-flavor jets in proton-proton collisions at $\sqrt{s}=13$ TeV." Physical Review D, 104 (3).

As Published: 10.1103/PHYSREVD.104.032006

Publisher: American Physical Society (APS)

Persistent URL: <https://hdl.handle.net/1721.1/142077>


Version: Final published version: final published article, as it appeared in a journal, conference proceedings, or other formally published context

Terms of use: Creative Commons Attribution 4.0 International license



Search for top squarks in final states with two top quarks and several light-flavor jets in proton-proton collisions at $\sqrt{s} = 13$ TeV

A. M. Sirunyan *et al.**
(CMS Collaboration)

 (Received 13 February 2021; accepted 28 June 2021; published 20 August 2021)

Many new physics models, including versions of supersymmetry characterized by R -parity violation (RPV), compressed mass spectra, long decay chains, or additional hidden sectors, predict the production of events with top quarks, low missing transverse momentum, and many additional quarks or gluons. The results of a search for new physics in events with two top quarks and additional jets are reported. The search is performed using events with at least seven jets and exactly one electron or muon. No requirement on missing transverse momentum is imposed. The study is based on a sample of proton-proton collisions at $\sqrt{s} = 13$ TeV corresponding to 137 fb^{-1} of integrated luminosity collected with the CMS detector at the LHC in 2016–2018. The data are used to determine best fit values and upper limits on the cross section for pair production of top squarks in scenarios of RPV and stealth supersymmetry. Top squark masses up to 670 (870) GeV are excluded at 95% confidence level for the RPV (stealth) scenario, and the maximum observed local signal significance is 2.8 standard deviations for the RPV scenario with top squark mass of 400 GeV.

DOI: [10.1103/PhysRevD.104.032006](https://doi.org/10.1103/PhysRevD.104.032006)

I. INTRODUCTION

Supersymmetry [1,2] (SUSY) is an extension of the standard model (SM) that may provide a solution to the gauge hierarchy problem [3]. In the SUSY framework, quadratically divergent radiative corrections to the Higgs boson mass parameter, dominated by loops involving the top quark, are canceled by loops with bosonic top quark superpartners (top squark, \tilde{t}). To avoid fine-tuning, the lightest \tilde{t} and the superpartners of the Higgs bosons (Higgsinos) must have masses near the weak scale [3–8] and could therefore have nonnegligible production cross sections at the CERN Large Hadron Collider (LHC).

Most searches for the \tilde{t} look for an excess of events with large missing transverse momentum p_T^{miss} originating from the undetected lightest SUSY particle (LSP) produced in \tilde{t} decays. It is typical in these searches to assume that the LSP is the lightest neutralino $\tilde{\chi}_1^0$, which is stable if R -parity [9] is conserved. However, it has been shown [10–12] that this search strategy is not sensitive to well-motivated SUSY models that predict signatures with low p_T^{miss} in models with gauge mediated SUSY breaking [13], compressed mass spectra [14,15], hidden valleys [16], or other

mechanisms. As searches performed at the LHC using events with high p_T^{miss} set ever more stringent lower bounds on the \tilde{t} mass [17–22], searches for low- p_T^{miss} alternatives become increasingly important.

Models of R -parity violating (RPV) SUSY produce low- p_T^{miss} signatures by providing a mechanism for the LSP, in this case $\tilde{\chi}_1^0$, to decay. Among other couplings, RPV SUSY includes a trilinear Yukawa coupling between quarks and squarks that allows the $\tilde{\chi}_1^0$ to decay into three quarks via an off shell squark [9]. These couplings are typically referred to as λ''_{ijk} where i, j , and k specify the generations of the participating (s)quarks. The benchmark RPV model used in this analysis is illustrated in Fig. 1. The \tilde{t} decays in the typical way into a top quark and a $\tilde{\chi}_1^0$, and the $\tilde{\chi}_1^0$ undergoes an RPV decay via nonzero λ''_{112} into three light-flavor quarks, $\tilde{\chi}_1^0 \rightarrow uds$. However, since this analysis does not distinguish between jets originating from quarks of the first and second generation, our results are more broadly applicable to any RPV model with coupling λ''_{abc} with $a, b, c \in \{1, 2\}$.

Stealth SUSY models [12,23,24] introduce a new hidden “stealth” sector of light particles with small or absent couplings to the SUSY breaking sector and finite couplings to the visible sector. Because of the weak connection to the SUSY breaking sector, SUSY is approximately conserved in the stealth sector, resulting in stealth particles that are nearly mass-degenerate with their superpartners. Production and decay of stealth particles via interactions with visible particles can be achieved through a variety of

*Full author list given at the end of the article.

Published by the American Physical Society under the terms of the [Creative Commons Attribution 4.0 International license](https://creativecommons.org/licenses/by/4.0/). Further distribution of this work must maintain attribution to the author(s) and the published article’s title, journal citation, and DOI. Funded by SCOAP³.

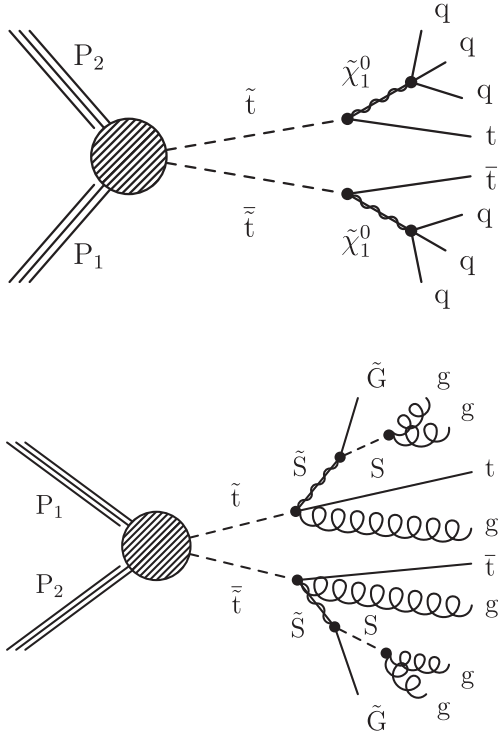


FIG. 1. Diagrams of top squark pair production with decays to top quarks and additional light-flavor quarks for the RPV SUSY model (upper) and with decays to top quarks and gluons for the stealth $SY\tilde{Y}$ model (lower).

“portals” including mediation by the Higgs boson or new particles at a higher mass scale. The benchmark stealth SUSY model used in the interpretation of the results of this search (stealth $SY\tilde{Y}$) [24] assumes a minimal stealth sector containing only one scalar particle S with even R -parity and its superpartner \tilde{S} , both of which are singlets under all SM interactions, and a portal mediated by loop interactions involving a new vectorlike messenger field (Y), the gluon (g), $\tilde{\chi}_1^0$, S , and \tilde{S} . Decays of the \tilde{t} in the stealth $SY\tilde{Y}$ model are illustrated in Fig. 1. Each \tilde{t} decays to a gluon, top quark, and \tilde{S} , with subsequent decays of \tilde{S} to S and a gravitino \tilde{G} and S to jets via $S \rightarrow gg$. Because of the small mass splitting between the S and \tilde{S} , as well as the small \tilde{G} mass, the undetected \tilde{G} carries away very little momentum. Thus, the stealth $SY\tilde{Y}$ model shares the general feature of all stealth SUSY models in that it naturally produces a low- p_T^{miss} signature without R -parity violation or a special tuning of sparticle masses.

The RPV and stealth $SY\tilde{Y}$ models are characterized by the masses of the particles and branching fractions in the decay chain. In the benchmark RPV model, we take the $\tilde{\chi}_1^0$ mass to be 100 GeV. For the benchmark stealth $SY\tilde{Y}$ model, the critical small \tilde{S} - S mass splitting is held constant at 10 GeV, and we assume a \tilde{S} mass of 100 GeV and a \tilde{G} mass of 1 GeV. For both models, a range of \tilde{t} masses ($m_{\tilde{t}}$) are

considered from 300 to 1400 GeV, and all decays described above are assumed to be prompt with unity branching fractions.

In this paper, we describe a search for \tilde{t} pair production followed by the decay of each \tilde{t} into a top quark and three light-flavor jets via the benchmark RPV and stealth $SY\tilde{Y}$ models described above. This is the first search of its kind at the LHC. Previous searches for RPV \tilde{t} decays focused on final states with dijet resonances [25,26], lepton-jet resonances [27,28], intermediate leptonic chargino decays [29], or final states with many b quarks [30]. Previous searches for stealth SUSY targeted superpartners of light-flavor quarks with decays into gauge bosons and jets [31,32]. Measurements of the $t\bar{t}$ differential production cross section have been reinterpreted in the context of RPV and stealth SUSY [24,33] and were found to yield weak constraints for the models considered in this paper.

Before describing each step in more detail in subsequent sections, we provide an overview of the analysis strategy here. The main distinguishing feature of the signals in this analysis, in addition to the presence of two top quarks, is high jet multiplicity (N_{jets}). The SM backgrounds arise through processes including top quark pair production ($t\bar{t}$), multijet production from quantum chromodynamics (QCD), production of $t\bar{t}$ in association with SM weak gauge bosons or additional top quarks ($t\bar{t} + X$), production of weak gauge bosons, and single top quark production (other). These SM processes all include additional jets from initial- and final-state radiation (ISR and FSR). The QCD background is primarily suppressed by requiring the presence of exactly one charged lepton (e or μ) arising from the leptonic decay of a top quark. Backgrounds that do not produce any top quarks are suppressed by requiring the presence of at least one jet identified as arising from the fragmentation of a bottom quark (b -tagged jet), and additionally that the invariant mass of the lepton and a b -tagged jet be consistent with the presence of a top quark.

The signal is distinguished from the dominant and irreducible $t\bar{t}$ background by means of a neural network (NN) trained to recognize differences in the spatial distribution of jets and decay kinematic distributions between signal and $t\bar{t}$ background events. Events are divided into 24 categories based on their NN score (S_{NN}) and N_{jets} ; categories with higher (lower) S_{NN} and N_{jets} tend to be signal enriched (depleted). We perform a simultaneous fit to the number of events in data in S_{NN} and N_{jets} categories to estimate the total numbers of $t\bar{t}$ and potential signal events present in the data, as well as the distribution of $t\bar{t}$ events in S_{NN} and N_{jets} categories. The NN output is designed to have no dependence on N_{jets} , so that the N_{jets} distribution of $t\bar{t}$ events can be constrained in the fit to be the same for all S_{NN} categories. This requirement for $t\bar{t}$ N_{jets} shape invariance is important for the analysis and will be discussed throughout the paper.

This paper is organized as follows. We introduce the CMS detector and methods for event reconstruction and selection in Sec. II. Samples of simulated events are described in Sec. III. The estimation and modeling of SM backgrounds are explained in Sec. IV, and the description of the treatment of systematic uncertainties is in Sec. V. Finally, the results and their interpretation are in Sec. VI, followed by the summary in Sec. VII.

II. EXPERIMENTAL TECHNIQUES

The search is performed using a data sample of proton-proton (pp) collisions at $\sqrt{s} = 13$ TeV, corresponding to an integrated luminosity of 137 fb^{-1} , collected in 2016–2018 with the CMS detector at the LHC. Data and simulation samples from four periods (2016, 2017, 2018A, 2018B) are treated separately in order to address variations in detector and LHC conditions. Data from 2018 are divided into two samples (2018A and 2018B), with 2018B corresponding to the period when a detector malfunction prevented readout from 3% of the hadron calorimeter. In this section, we define reconstructed physics objects and describe the selection criteria for events in the signal region (SR) and the control region (CR) of the analysis.

The central feature of the CMS apparatus is a superconducting solenoid of 6 m internal diameter, providing a magnetic field of 3.8 T. Within the solenoid volume are a silicon pixel and strip tracker, a lead tungstate crystal electromagnetic calorimeter, and a brass and scintillator hadron calorimeter, each composed of a barrel and two end cap sections. Forward calorimeters extend the pseudorapidity coverage provided by the barrel and end cap detectors. Muons are detected in gas-ionization chambers embedded in the steel flux-return yoke outside the solenoid. A more detailed description of the CMS detector, together with a definition of the coordinate system used and the relevant kinematic variables, can be found in Ref. [34].

The CMS trigger system is described in Ref. [35]. Events are selected using triggers that require the presence of at least one electron or one muon. The minimum transverse momentum p_T threshold is 27 (35) GeV for electrons and 24 (24) GeV for muons in 2016 (2017–2018). The triggers at these thresholds require the lepton to be isolated from tracks and calorimeter deposits in the detector. Events may also be selected from single-lepton triggers with higher p_T thresholds, 115 GeV for electrons and 50 GeV for muons, with no isolation requirements. The combined trigger efficiency varies from 80% for leptons with p_T close to the lower thresholds to greater than 95% for leptons with $p_T > 120$ GeV.

Events are reconstructed using the particle-flow (PF) algorithm [36], which reconstructs particles in an event using an optimized combination of information from the various elements of the CMS detector and identifies each as a photon, electron, muon, charged hadron, or neutral

hadron. These particles are further clustered into jets as described below.

The reconstructed vertex with the largest value of summed physics-object p_T^2 is taken to be the primary pp interaction vertex, where the physics objects are the jets, clustered using the anti- k_T algorithm [37,38] with the charged-particle tracks assigned to the vertex as inputs, and the associated missing transverse momentum, taken as the negative vector sum of the p_T of those jets [39]. Charged-particle tracks associated with vertices from other pp interactions (pileup) are removed from further consideration. The primary vertex is required to lie within 24 cm of the interaction point along the beam axis, and within 2 cm in the plane transverse to the beam axis.

Electrons and muons must satisfy $p_T > 30$ GeV and $|\eta| < 2.4$. For the analysis of the 2017 and 2018 data, the electron p_T threshold is increased to 37 GeV to account for the higher trigger threshold. The lepton identification requirements are the “tight” criteria for electrons [40] and the “medium” criteria for muons [41]. Leptons must be isolated within a cone of radius $R = \sqrt{(\Delta\phi)^2 + (\Delta\eta)^2}$ that scales as $1/p_T$ between a maximum of 0.2 for leptons with $p_T < 50$ GeV and a minimum of 0.05 for lepton $p_T > 200$ GeV [42].

Jets are clustered from the reconstructed PF particles using the anti- k_T algorithm with a distance parameter of 0.4. Criteria are applied to remove events with jets arising from instrumental effects or reconstruction failures [43,44]. The reconstructed jet energies are corrected for the non-linear response of the detector [45,46] and for contributions from neutral hadrons from pileup [47]. Jets are required to have $p_T > 30$ GeV and $|\eta| < 2.4$. Jets overlapping with a selected lepton within a cone of radius $R = 0.4$ are removed. A neural network-based algorithm [48] is used to identify b quark jets; for jets with p_T around 30 GeV, the algorithm has an efficiency of 65% and a misidentification rate for light-flavor jets (including gluon jets) of 1%.

In addition to the trigger and vertex criteria above, events in the SR must contain exactly one isolated electron or muon and at least seven jets, at least one of which should be b tagged. Samples with seven and eight jets include a small number of expected signal events but are included in the SR to constrain the background. To further reject the QCD background, we require the scalar sum of jet p_T (H_T) to exceed 300 GeV. To suppress non- $t\bar{t}$ backgrounds, we require the invariant mass of the system formed by the b -tagged jet and the lepton to be between 50 and 250 GeV. If there is more than one b -tagged jet in the event, the invariant mass of each b -tagged jet and the lepton is considered, and at least one combination is required to meet the above criterion. No requirement is made on the event p_T^{miss} .

In addition to the SR, a signal-depleted control region (CR) dominated by QCD background is defined with the dual purpose of determining the QCD contribution to the

SR and verifying the important assumption of $t\bar{t} N_{\text{jets}}$ shape invariance with S_{NN} . Despite being dominated by QCD background, the CR is useful for confirming $t\bar{t} N_{\text{jets}}$ shape invariance because many of the jets used as inputs to the NN arise from QCD radiation, which is common to the $t\bar{t}$ and QCD backgrounds; this claim is verified in Sec. V. The CR is defined similarly to the SR with the differences being that the lepton is required to be a muon; the muon is required to fail the SR isolation requirement; there is no requirement for a b -tagged jet, nor on the invariant mass of the lepton and b -tagged jet; the only trigger used is the high-threshold muon trigger without an isolation requirement; and the muon p_{T} threshold is 55 GeV.

III. SIMULATED EVENT SAMPLES

Simulated event samples are used in the estimation of the expected number of SM background and signal events passing the SR selection. Top quark pair and single top quark events produced in the t channel are generated with the next-to-leading-order (NLO) POWHEG v2.0 [49–53] generator, while single top quark events in the $t\bar{W}$ channel are generated with POWHEG v1.0 [52]. Single top quark production in the s channel, as well as rare SM processes such as $t\bar{t}Z$ and $t\bar{t}W$ are generated at NLO accuracy with the MadGraph 5_aMC@NLO v2.2.2 program. The MadGraph 5_aMC@NLO v2.2.2 generator [54,55] is used in the leading-order (LO) mode to simulate QCD and $W + \text{jets}$ events.

For the signal, top squark pair production events are generated using MadGraph 5_aMC@NLO in LO mode, including up to two additional partons in the matrix element calculation. The top squarks are decayed using PYTHIA v8.212 (2016) or 8.226 (2017–2018) [56] according to the signal models described in Sec. I. The signal production cross section ($\sigma_{\bar{t}\bar{t}}$) is calculated as a function of $m_{\bar{t}}$ using approximate next-to-NLO (NNLO) plus next-to-next-to-leading-logarithm (NNLL) calculations [57,58].

The generation of these processes is based on either LO or NLO parton distribution functions (PDFs) using NNPDF3.0 [59] for the simulated samples corresponding to 2016 detector conditions and using the NNLO PDF sets from NNPDF3.1 [60] for the 2017 and 2018 simulated samples. Parton showering and hadronization are simulated with PYTHIA using underlying event tune CUETP8M1 [61] for 2016 samples, except for $t\bar{t}$ production which used tune CUETP8M2T4 [62], or PYTHIA with tune CP5 (CP2) [63] for all 2017 and 2018 background (signal) samples. To model the effects of pileup, simulated events are generated with a nominal distribution of pp interactions per bunch crossing and then reweighted to match the corresponding distribution in data. The CMS detector response is simulated using a GEANT4-based model [64], and event reconstruction is performed in the same manner as for collision data. The most precise cross section calculations available are used to normalize the SM

simulated samples, corresponding to NLO or NNLO accuracy in most cases [54,65–71].

The simulation is corrected to eliminate small discrepancies between data and simulation in the trigger efficiency, lepton selection efficiency, and b tagging efficiency. Analysis-specific corrections for the H_{T} distribution in $t\bar{t}$ simulation, parametrized as functions of N_{jets} and H_{T} , are obtained in a signal-depleted sample identical to the SR, except for the requirement $5 \leq N_{\text{jets}} \leq 7$. Events with $N_{\text{jets}} = 7$ are common to the SR, but as mentioned above, this sample has low signal contamination. The correction is parametrized with an exponential function in H_{T} with parameters depending linearly on N_{jets} in order to extend the correction into the $N_{\text{jets}} > 7$ SR. The H_{T} correction is small at low H_{T} and 20%–40% at $H_{\text{T}} = 1500$ GeV, depending on N_{jets} .

IV. BACKGROUND ESTIMATION

Simulated background events passing the SR selection requirements predominantly originate from $t\bar{t}$ production, with contributions of less than 10% from QCD, and a few percent from the remaining minor backgrounds including $t\bar{t}$ production in association with a vector boson, single top quark production, and $W + \text{jets}$.

As introduced in Sec. I, the crux of the analysis is to estimate the dominant $t\bar{t}$ background in four bins of S_{NN} and six N_{jets} bins using a simultaneous binned maximum-likelihood fit constraining the $t\bar{t} N_{\text{jets}}$ shape to be the same in all S_{NN} categories. Event yields, as well as the N_{jets} and S_{NN} distributions, are fixed at values determined from a signal-depleted data control sample for the QCD background and from simulation for the minor backgrounds, as described later in this section. The yield and N_{jets} shape of the $t\bar{t}$ background, along with the signal strength, are determined in the fit; signal strength is defined as the ratio of the fit signal event yield to the one predicted by SUSY.

The NN is trained to discriminate between signal and $t\bar{t}$ background by exploiting differences in the event shape and distributions of the kinematic variables. The gradient reversal technique [72] is used to minimize dependence of the NN output on N_{jets} , as required by the primary assumption that the $t\bar{t} N_{\text{jets}}$ shape is the same in all S_{NN} categories. All NN input variables are computed in an approximate center-of-mass frame defined by all jets in the event with $p_{\text{T}} > 30$ GeV and $|\eta| < 5$. The NN input variables include the four-vector components for the seven jets in the event with the highest momentum in the center-of-mass frame, the four-vector components of the lepton in the event, the second through fifth Fox-Wolfram moments [73] normalized by the first moment, and the three eigenvalues of the sphericity tensor [74] normalized by the sum of the eigenvalues. The Fox-Wolfram moments and sphericity tensor eigenvalues, which are computed from the same seven highest momentum jets, quantify the

distribution of jet energy in the event, which tends to be more spherical for signal $\tilde{t}\tilde{t}$ pair production than for the $t\bar{t}$ background.

For the NN training, simulated $t\bar{t}$ events are used for the background sample, and a mixture of RPV and stealth $SY\bar{Y}$ simulated events with $m_{\tilde{t}}$ from 350–850 GeV is used as the signal sample. In this way, the NN can identify common features among all signal samples ensuring a search with broad sensitivity. Reflecting differences in simulation between the data taking periods, as described in Sec. III, a single training is used for 2017, 2018A, and 2018B, with a separate training used for 2016. The S_{NN} distributions for the simulated background, several signal models, and the 2016 and 2017 + 2018 data are shown in Fig. 2.

For each of the six N_{jets} bins, events are divided into four S_{NN} bins: $S_{\text{NN},1}$ (lowest S_{NN}), ..., $S_{\text{NN},4}$ (highest S_{NN}). The S_{NN} bin boundaries are chosen separately for each N_{jets} bin such that the expected significance for the 550 GeV RPV signal model, which has expected significance close to 5 standard deviations (σ), is maximized, under the constraint that the fraction of simulated $t\bar{t}$ events in each S_{NN} bin is the same for all N_{jets} bins. For example, the fraction of all events in each N_{jets} bin falling into the $S_{\text{NN},1}$ bin is constrained to be approximately 56%, while the fraction of events falling into the $S_{\text{NN},4}$ bin is constrained to be approximately 2.4%. This constraint removes the small dependence of S_{NN} on N_{jets} that remains after NN training with gradient reversal.

In the maximum-likelihood fit, the $t\bar{t}$ N_{jets} distribution is parametrized with a function inspired by QCD jet scaling patterns [75] in which the ratio $R(i) = M_{i+1}/M_i$, where M_i is the number of events with $N_{\text{jets}} = i$, can be described by a falling ‘‘Poisson’’ component at low N_{jets} and a constant ‘‘staircase’’ component at high N_{jets} . This ratio is well modeled by the function,

$$f(i) = a_2 + \left[\frac{(a_1 - a_2)^{i-7}}{(a_0 - a_2)^{i-9}} \right]^{1/2}.$$

Notice that $a_0 = f(7)$, $a_1 = f(9)$, and a_2 is the asymptotic value for large i . This particular parametrization was chosen to avoid large correlations between the fit parameters. The N_{jets} distribution for each S_{NN} bin j (see Fig. 4) is modeled using a recursive expression given by $M_i^j = Y_7^j \prod_{k=7}^{i-1} f(k)$ where Y_7^j are normalization parameters that are floating in the fit. The last N_{jets} bin considered is an inclusive $N_{\text{jets}} \geq 12$ bin, such that $i \in [7, 12]$. In the maximum-likelihood fit, the free parameters consist of the three shape parameters a_0 , a_1 , and a_2 ; the four normalization parameters Y_7^j ; the signal strength; and all nuisance parameters related to systematic uncertainties described in Sec. V.

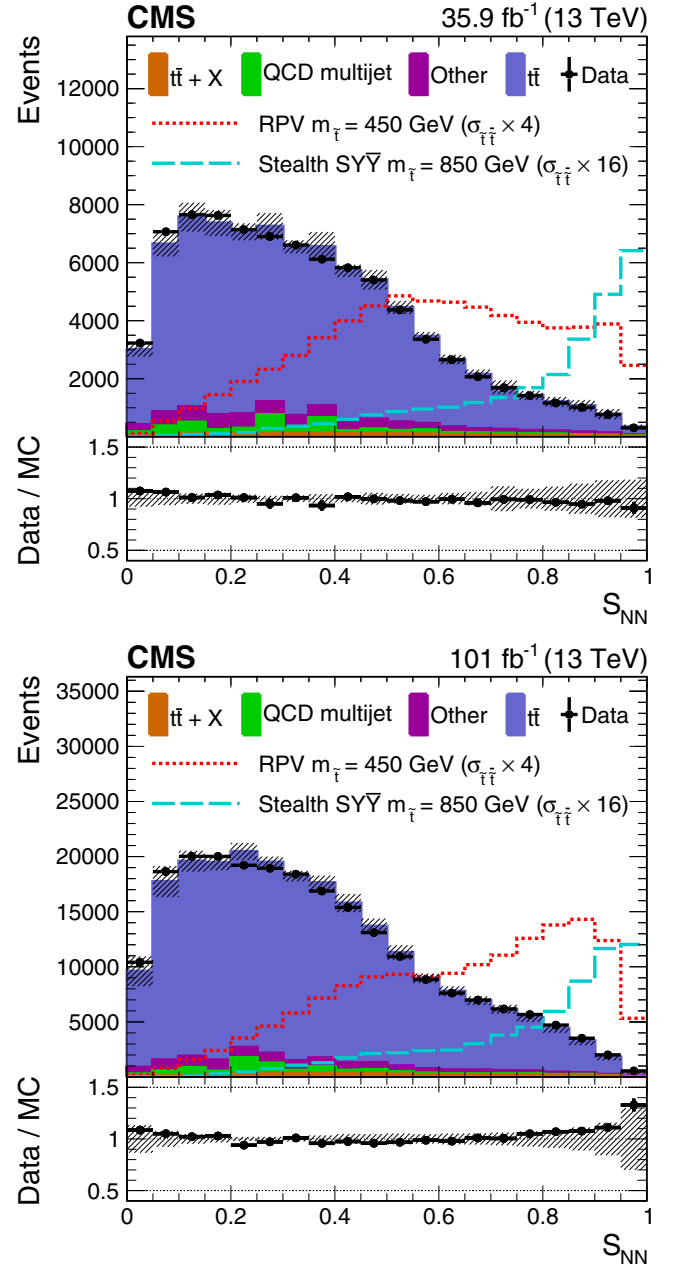


FIG. 2. The S_{NN} distributions for the 2016 training (upper) and 2017 + 2018 training (lower) show the corresponding data in the SR (black points); simulated background normalized to the number of data events (filled histograms); RPV signal model with $m_{\tilde{t}}$ of 450 GeV (red short dashed); and stealth $SY\bar{Y}$ signal model with $m_{\tilde{t}}$ of 850 GeV (cyan long dashed). All events shown pass the SR event selection. The band on the total background histogram denotes the dominant systematic uncertainties related to the modeling of H_T , jet mass, and jet p_T in the $t\bar{t}$ simulation, as well as the statistical uncertainty for the non- $t\bar{t}$ components. The lower panel shows the ratio of the number of data events to the number of normalized simulated events with the band representing the difference between the nominal ratio and the ratio obtained when varying the total background by its uncertainty.

The QCD background yield parameters are fixed in the fit at the values determined from the CR. More specifically, the QCD background prediction for each $N_{\text{jets}}\text{-}S_{\text{NN}}$ bin in the SR is given by the yield for the same bin in the CR in data, after subtraction of the non-QCD backgrounds as predicted from simulation, multiplied by the ratio of SR to CR yields in simulation (R_{QCD}). This procedure is verified with a closure test in the simulation. The yield parameters from the minor backgrounds are also kept fixed in the fit at the values predicted by simulation. While the yield parameters are fixed in the fit, the ultimate contributions from QCD and minor backgrounds vary according to the constrained nuisance parameters related to systematic uncertainties in those fit components.

V. SYSTEMATIC UNCERTAINTIES AND FIT VALIDATION

As described in Sec. IV, an unbiased estimate of the dominant $t\bar{t}$ background is obtained from the fit to data as long as the $t\bar{t}$ N_{jets} shape is the same for all four S_{NN} bins. By construction, N_{jets} shape invariance is achieved in the simulation with an N_{jets} -specific S_{NN} binning as described in the previous section. Thus, systematic uncertainties on the $t\bar{t}$ background are important to the degree that they violate the assumption that the S_{NN} binning determined in simulation also applies to the data. We quantify how each source of uncertainty causes deviations from the assumed N_{jets} shape invariance by comparing the nominal N_{jets} shape to the N_{jets} shapes in all S_{NN} bins after performing the relevant systematic variation to the $t\bar{t}$ simulation. Each systematic variation is associated with a constrained nuisance parameter in the fit. The deviation in shape for each N_{jets} distribution, derived from the ratio of the postvariation shape divided by the nominal shape, changes linearly with the associated nuisance parameter for the systematic variation, while preserving the normalization of the distribution.

Sources of $t\bar{t}$ shape uncertainty include uncertainty in aspects of event generation including PDFs, choice of renormalization and factorization scales (μ_{R} , μ_{F} scales), and parton shower modeling, which is itself composed of aspects related to modeling of ISR, FSR, color reconnection in the parton shower, matrix element-parton shower matching scale (ME-PS), underlying event (UE tune), and pileup modeling. The uncertainty due to the choice in (μ_{R} , μ_{F}) scales is determined by independently varying both by factors of 2.0 and 0.5 excluding the variations (2.0, 0.5) and (0.5, 2.0) [55,76,77]. The ISR and FSR uncertainties originate from variations of the renormalization scale for the parton shower by factors 0.5 and 2.0, effectively varying the value of α_{S} . The color reconnection uncertainty is calculated by allowing resonant decays to occur before the merging of multi-parton systems. The ME-PS uncertainty is obtained by varying the POWHEG parameter that

governs ME-PS matching about its nominal value according to $h_{\text{damp}} = 1.379^{+0.926}_{-0.505}$ times the top quark mass [63]. The UE tune uncertainty comes from variation of the PYTHIA parameters that control the modeling of the underlying event as described in Ref. [63]. The total inelastic pp cross section is changed by 5% to estimate the uncertainty related to pileup [78].

Sources of $t\bar{t}$ shape uncertainty related mostly to aspects of detector simulation include determination of jet energy scale (JES) and resolution (JER), modeling of the b tagging efficiency, modeling of the efficiency for lepton triggers, identification, and isolation (lepton efficiencies); residual mismodeling of H_{T} , jet p_{T} , and jet mass; and use of the CR for measuring deviations from the assumption of N_{jets} shape invariance.

The uncertainty in the modeling of H_{T} in the $t\bar{t}$ simulation is composed of four separate components. The first H_{T} uncertainty (primary) is taken as the full difference in the $t\bar{t}$ background shape with and without the H_{T} correction. The second H_{T} uncertainty (validation) is taken as the difference between the simulation with nominal H_{T} correction (described in Sec. III) and the observed H_{T} distribution in the signal-depleted SR sample with $N_{\text{jets}} = 8$. The third and fourth H_{T} uncertainties address the choices of parameterization of the H_{T} correction as functions of H_{T} and N_{jets} . For these, we take the uncertainty as the difference between the nominal correction and two alternate corrections that use the $H_{\text{T}} = 2000$ GeV correction for all events with $H_{\text{T}} > 2000$ GeV (H_{T} -parametrization) and the $N_{\text{jets}} = 7$ correction for all values of N_{jets} (N_{jets} -parametrization).

Comparisons of data and simulation in the CR show that the simulation predicts distributions with higher values of jet p_{T} and mass than observed. The observed discrepancy at jet p_{T} (mass) of 400 (50) GeV depends on jet p_{T} rank and is small for the highest p_{T} jet in each event growing to approximately 50% for the jet with sixth-highest p_{T} in each event. Similar trends are observed in the signal-depleted, $t\bar{t}$ -dominated SR with $N_{\text{jets}} = 7$. In the CR, the discrepancy in the falling tail of each distribution is minimized when the p_{T} (mass) of each jet is scaled by the value 0.95, 0.95, 0.95, 0.95 (0.95, 1.01, 0.98, 0.98) for 2016, 2017, 2018A, and 2018B, respectively. Thus, the related $t\bar{t}$ shape uncertainty is taken to be the resulting difference between scaled and nominal simulated $t\bar{t}$ distributions. The dependence on jet p_{T} rank indicates that the discrepancy arises predominantly in the event generation; however, we choose to estimate the associated systematic uncertainty separately for each data taking period to include potential effects of detector response simulation. The H_{T} correction is omitted from the determination of these jet p_{T} and mass uncertainties to avoid double counting of H_{T} mismodeling effects. In addition, because the estimation of jet p_{T} and mass uncertainties relies on variable scaling (rather than event reweighting), the uncertainties include effects of

changes in the S_{NN} for each event, which is not included in the H_T uncertainty.

As mentioned above, the use of N_{jets} -dependent S_{NN} binning ensures that the N_{jets} shape is the same in all four S_{NN} bins in simulation, and the use of the same binning in the data assumes that the $N_{\text{jets}}-S_{\text{NN}}$ dependence is well modeled in the simulation. This assumption is confirmed and a related systematic uncertainty is determined by comparing the N_{jets} shapes (in five uniform S_{NN} bins) for data and simulation in the CR. For each of the six N_{jets} bins, we compute the ratio $R_M = (1/\mu_i)(M_{\text{all}}/M_i)$ as a

function of S_{NN} , where M_{all} is the total number of events in all N_{jets} bins, M_i is the total number of events in the $N_{\text{jets}} = i$ bin, and μ_i is the uncertainty-weighted average of M_{all}/M_i in the $N_{\text{jets}} = i$ bin used to facilitate comparison of the R_M shapes between samples and N_{jets} bins with different normalizations. Figure 3 shows a comparison of R_M (from $N_{\text{jets}} = 7$ and 11 in the 2016 analysis) for simulation of the QCD background in the CR ($\text{QCD}_{\text{CR}}^{\text{MC}}$), simulation of $t\bar{t}$ in the SR ($t\bar{t}_{\text{SR}}^{\text{MC}}$), and the data in the QCD background-dominated CR (Data_{CR}). Agreement between $\text{QCD}_{\text{CR}}^{\text{MC}}$ and $t\bar{t}_{\text{SR}}^{\text{MC}}$ demonstrates that QCD background-dominated data in the CR are a good proxy for $t\bar{t}$ -dominated data in the SR, and agreement between $\text{QCD}_{\text{CR}}^{\text{MC}}$ and Data_{CR} verifies that the dependence of the N_{jets} shape on S_{NN} is well modeled in the simulation. Similar agreement is found for the R_M distributions for the other N_{jets} bins and data periods. The uncertainty related to the combination of both effects is taken as the difference between $t\bar{t}_{\text{SR}}^{\text{MC}}$ and Data_{CR} .

TABLE I. Summary of the impact of systematic uncertainties in the expected event yields for the $t\bar{t}$ background, minor backgrounds (both $t\bar{t} + X$ and other), and the RPV signal model with $m_{\tilde{t}} = 550$ GeV. Abbreviated names for each source of uncertainty are explained in the text. For sources of uncertainty for which the size of the impact depends on N_{jets} and S_{NN} , a representative range of values showing the 16th and 84th percentile of all the corrections is listed with the maximum value from all bins shown in parentheses. All values are in units of percent.

Source of uncertainty	$t\bar{t}$ background	Minor background	RPV signal
PDFs	0–1 (2)	0–1 (8)	0–2 (7)
(μ_R, μ_F) scales	0–2 (5)	1–8 (18)	0–3 (4)
ISR	0–4 (15)
FSR	0–8 (27)
Color reconnection	0–10 (44)
ME-PS	0–14 (82)
UE tune	0–7 (100)
Pileup	0–2 (7)	0–7 (28)	0–2 (4)
JES	0–4 (18)	5–21 (100)	1–11 (31)
JER	0–2 (10)	1–15 (100)	0–6 (14)
b tagging	0–1 (3)	0–2 (12)	0–2 (2)
Lepton efficiencies	0–1 (1)	3–5 (5)	3–4 (4)
H_T primary	0–5 (17)
H_T validation	0–1 (4)	0–6 (10)	...
$H_T H_T$ - parametrization	0–2 (9)
$H_T N_{\text{jets}}$ - parametrization	0–7 (27)
Jet p_T	0–4 (15)
Jet mass	0–4 (15)
N_{jets} shape invariance	0–12 (37)
Integrated luminosity	...	2.3–2.5	2.3–2.5
Theoretical cross section	...	30	...

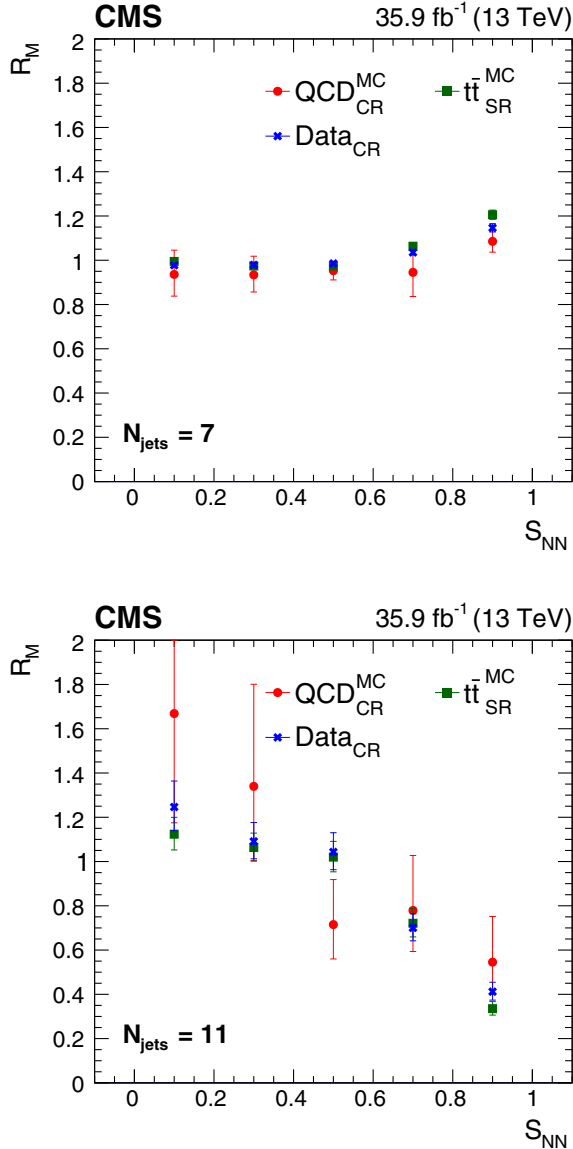


FIG. 3. Distribution in S_{NN} of the ratio R_M , as defined in the text, for $N_{\text{jets}} = 7$ (upper) and 11 (lower), for the QCD CR simulation (red circles), the $t\bar{t}$ SR simulation (green squares), and data in the CR (blue crosses) for the 2016 data period. The error bars indicate the statistical uncertainty in the value of R_M .

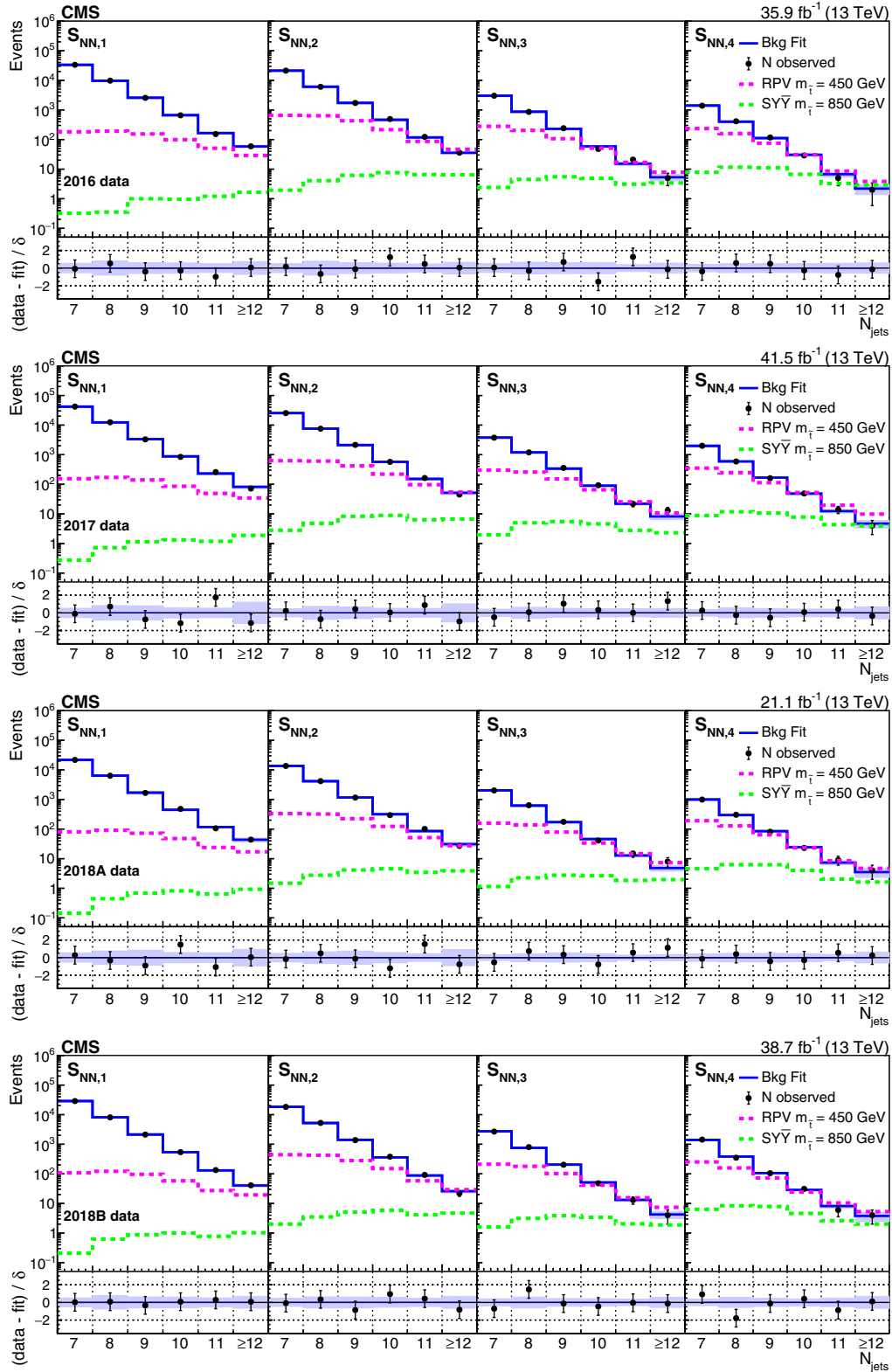


FIG. 4. Fitted background prediction and observed data counts for 2016, 2017, 2018A, and 2018B (from upper to lower rows) as functions of N_{jets} in each of the four bins in S_{NN} . The signal distributions normalized to the predicted cross section for the RPV model with $m_{\tilde{t}} = 450$ GeV and the stealth $SY\tilde{Y}$ model with $m_{\tilde{t}} = 850$ GeV are shown for comparison. The lower panel of each plot displays the difference between the number of observed events and the number of events determined by the fit divided by the statistical uncertainty associated with the observed number of events (δ) as black points with error bars denoting δ . The blue band shows the total systematic uncertainty in the fit from all nuisance parameters.

For the QCD background, the shape is obtained from data in the CR, and the normalization is set with R_{QCD} . Because the systematic uncertainties in the simulation largely cancel in the R_{QCD} ratio, the uncertainty in R_{QCD} is dominated by the statistical uncertainty of simulated samples and ranges from 15%–25% depending on data collection period.

Sources of systematic uncertainty in the predictions for signals and the minor backgrounds include PDFs, JES, JER, b tagging efficiency, lepton efficiency, trigger efficiency, (μ_R, μ_F) scales, cross sections for the minor backgrounds, and a 2.3%–2.5% uncertainty in the integrated luminosity [79–81]. Since the signal and minor backgrounds are estimated directly from simulation, related uncertainties are included as the full effect of the systematic variation on the yields in each N_{jets} and S_{NN} bin, thereby taking into account normalization effects as well as shape changes.

Uncertainties derived from comparisons of data and simulation separately in each data taking period (related to pileup, JES, JER, b tagging efficiency, lepton efficiencies, H_T corrections, N_{jets} shape invariance, and integrated luminosity) are treated as uncorrelated among all data samples. Uncertainties related to parton shower modeling are treated as fully correlated for 2017, 2018A, and 2018B, while the corresponding uncertainties for 2016 are

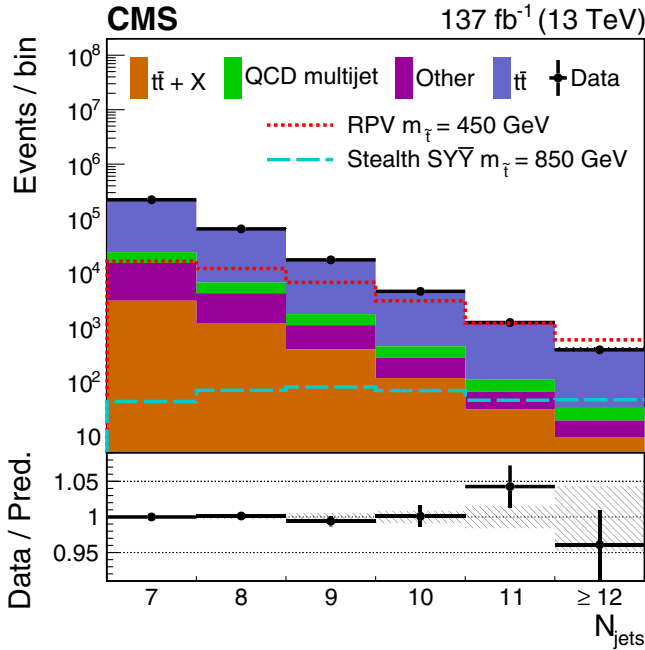


FIG. 5. Background prediction from the background-only fit and observed data counts as a function of N_{jets} summed over data periods and S_{NN} bins. Overlaid are expected distributions for the RPV and stealth $SY\tilde{Y}$ models with $m_{\tilde{t}} = 450$ and 850 GeV, respectively, normalized according to the top squark pair production cross section. For visualization purposes, the hatched band in the lower panel shows the quadrature sum of all of the uncertainties on the background prediction.

uncorrelated with those from the other data taking periods; uncertainties related to (μ_R, μ_F) scales and cross sections for the minor backgrounds are treated as correlated between all four periods.

Table I shows the impact of the systematic uncertainties on the expected event yields for the $t\bar{t}$ background, minor backgrounds, and the RPV signal model with $m_{\tilde{t}} = 550$ GeV. For sources of uncertainty for which the size of the impact depends on N_{jets} and S_{NN} , a representative range of values is listed along with the maximum value from all bins.

VI. RESULTS AND INTERPRETATION

The results of the fit to 2016, 2017, 2018A, and 2018B datasets with the signal strength fixed to zero (background-only fit) are shown along with the observed number of events in Fig. 4; each column (row) in the plot array

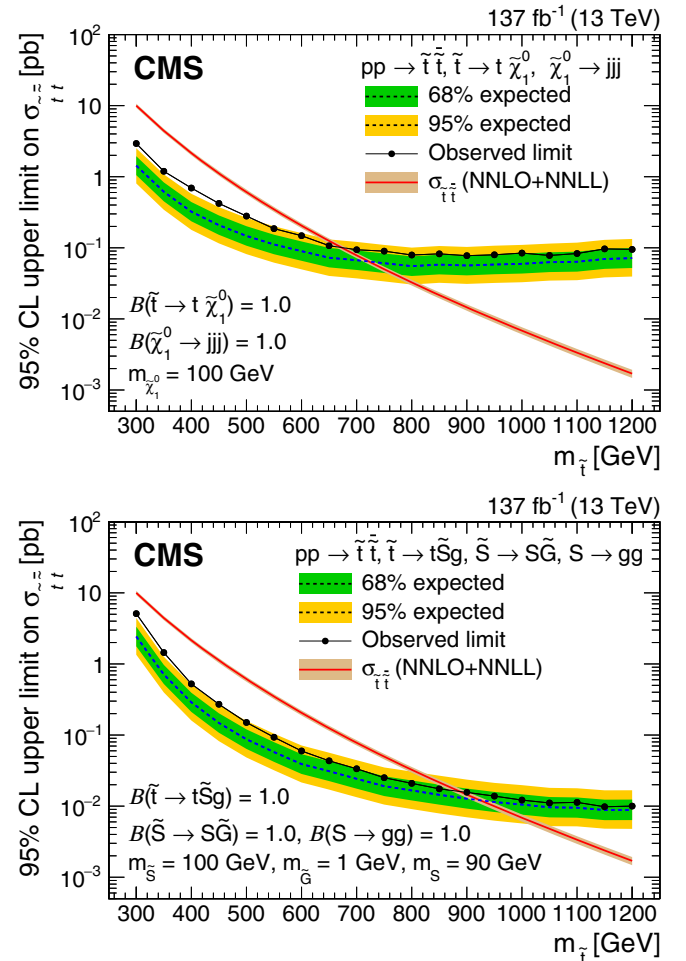


FIG. 6. Expected and observed 95% CL upper limit on the top squark pair production cross section as a function of the top squark mass for the RPV (upper) and stealth $SY\tilde{Y}$ (lower) SUSY models. Particle masses and branching fractions assumed for each model are included on each plot. The expected cross section computed at NNLO + NNLL accuracy is shown in the red curve.

corresponds to a specific S_{NN} bin (dataset). The expected distributions for top squark pair production in the specific RPV ($m_{\tilde{t}} = 450$ GeV) and stealth $SY\bar{Y}$ models ($m_{\tilde{t}} = 850$ GeV) described in Sec. I are overlaid for illustration purposes. The lower panel of each plot displays the difference between the observed number of events and the total number of expected events determined by the fit divided by the statistical uncertainty associated with the observed number of events (δ) as black points with error bars denoting δ . The blue band shows the total uncertainty in the fit determined from the full fit covariance matrix in order to account for the correlations among fit parameters. Figure 5 shows the results of the same background-only fit summed over S_{NN} bins and data periods with separate contributions from each background.

The data are also used to determine the 95% confidence level (CL) upper limits on $\sigma_{\tilde{t}\tilde{t}}$ and the signal strength p -values [82] for both the RPV and stealth $SY\bar{Y}$ models obtained using the CL_s approach [83–85] with asymptotic formulas [86] and the profile likelihood ratio as the test statistic. Figure 6 shows the expected and observed cross section limits as a function of $m_{\tilde{t}}$ for the benchmark RPV and stealth $SY\bar{Y}$ signal models. Comparing to the predicted cross section, these limits correspond to the exclusion of top squark masses in the range 300–670 and 300–870 GeV for the benchmark RPV and stealth $SY\bar{Y}$ models, respectively. Figure 7 shows the local p -value [82] of the signal strength, as a function of $m_{\tilde{t}}$, obtained from fits to the data

with each signal strength as a free parameter for both the RPV and stealth $SY\bar{Y}$ models. The p -value quantifies the probability for the background to produce an upward fluctuation at least as large as that observed. Fits are performed and p -values obtained separately for each dataset, as well as in a simultaneous fit to all datasets. We observe the most extreme p -value to be 0.003, which corresponds to a local significance of 2.8σ and a best fit signal strength of 0.21 ± 0.07 for the RPV model with $m_{\tilde{t}} = 400$ GeV assuming unity branching fractions for the decays described in Sec. I.

The 2.8σ local significance for the RPV model with $m_{\tilde{t}} = 400$ GeV is understood to arise from a combination of two effects. First, although the level of agreement between the observed data and the background expectation shown in Fig. 4 is reasonable, the agreement improves when the signal is included in the fit, contributing approximately 1.1σ to the significance. Second, the constrained nuisance parameters (NP) are pulled less from their initial values when the signal is included in the fit, contributing approximately 1.7σ to the significance. This second effect is illustrated in Fig. 8 which shows for each of a selection of NP: the fit value (θ) and uncertainty (δ_θ) from both the background-only fit (b) and the signal + background fit (s + b), as well as the $\Delta\chi^2 \equiv \chi^2(s + b) - \chi^2(b)$ difference of $\chi^2 \equiv (\theta/\delta_\theta)^2$ from the two fits. A θ value of one indicates that the fit value of the nuisance parameter is 1 standard deviation from its nominal value, and a δ_θ value less than one shows that the uncertainty is

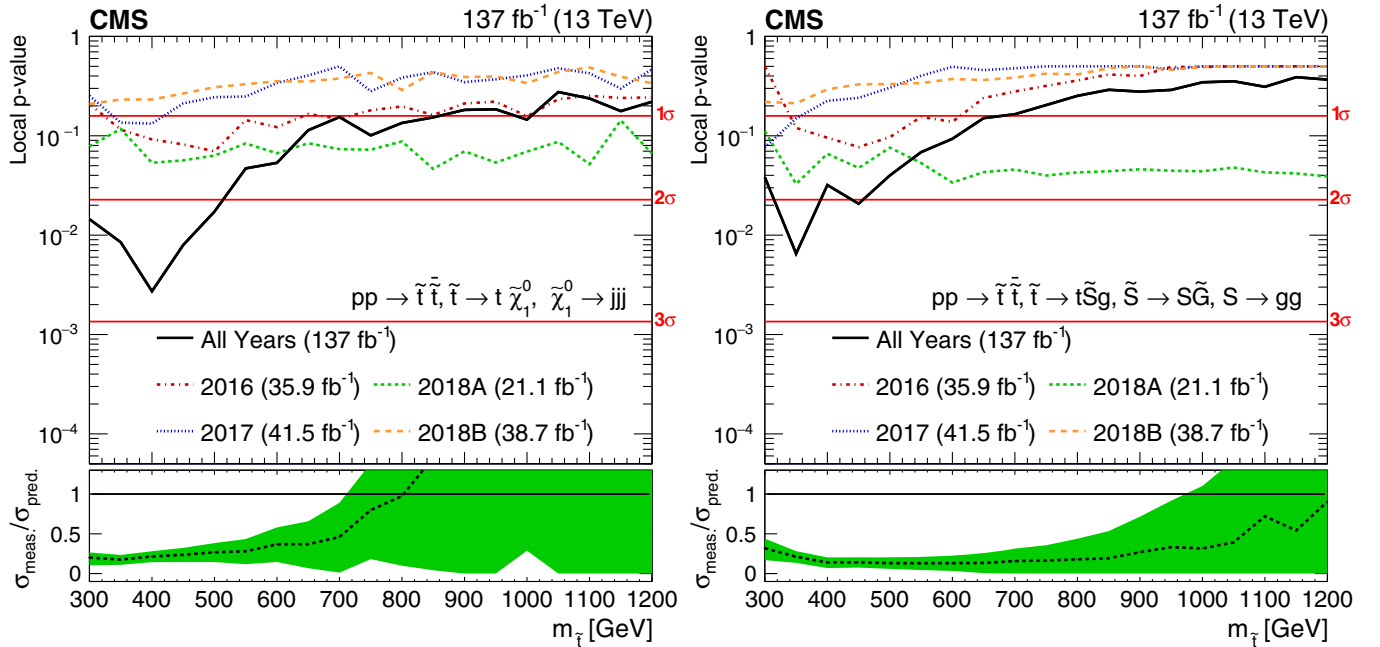


FIG. 7. Local p -value as a function of top squark mass for the RPV (left) and stealth $SY\bar{Y}$ models (right). The colored lines show the p -values for separate fits of the 2016 (red dash dotted), 2017 (blue dotted), 2018A (green short dashed), and 2018B (orange long dashed) datasets; the black line shows the p -value for the simultaneous fit of datasets. The lower panels show the best fit signal strength ($\sigma_{\text{meas}}/\sigma_{\text{pred}}$) as a function of top squark mass with uncertainty denoted by the green band.

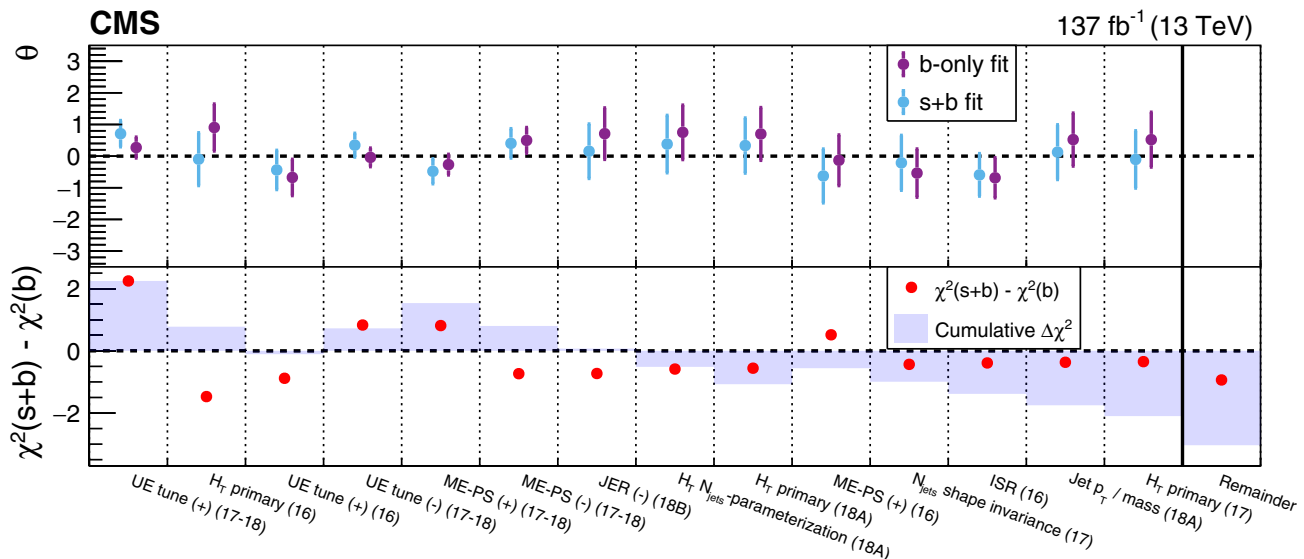


FIG. 8. The upper panel shows the fit values (θ) and uncertainties (δ_θ) for a selection of nuisance parameters (NP) from both the background-only fit (purple) and signal + background fit (blue) for the RPV model with $m_{\tilde{t}} = 400$ GeV. The x-axis labels refer to the NP sources described in Sec. V, the data period (16, 17, etc.), and the direction of variation (+, -). The lower panel shows the $\Delta\chi^2 \equiv \chi^2(s+b) - \chi^2(b)$ difference of $\chi^2 \equiv (\theta/\delta_\theta)^2$ from the signal + background (s + b) and background-only (b) fits as a red point for each NP and the cumulative sum of $\Delta\chi^2$ from left to right as a blue shaded histogram. The fourteen selected NP are those with $|\Delta\chi^2| > 0.3$, and the NP are ordered from left to right by decreasing $|\Delta\chi^2|$. The rightmost bin, separated by a vertical solid line, shows the sum of $\Delta\chi^2$ for all NP not displayed in the figure (red point) and the sum of $\Delta\chi^2$ for all NP (blue shaded histogram).

reduced in the fit relative to its initial value. All NPs have θ values below one for the background-only fit, and several NPs related to $t\bar{t}$ modeling are constrained with δ_θ in the range of 0.25–0.40. Figure 8 also shows the cumulative and total sums of $\Delta\chi^2$ for the NPs, with the sum for all NP of $\sum \Delta\chi^2 = -3.0$ corresponding to an approximate contribution to the signal significance of $\sqrt{|\sum \Delta\chi^2|} = 1.7\sigma$.

VII. SUMMARY

A first of its kind search for top squark pair production with subsequent decay characterized by two top quarks, additional gluons or light-flavor quarks, and low missing transverse momentum (p_T^{miss}) is described. Events containing exactly one electron or muon and at least seven jets, of which at least one should be b tagged, are selected from a sample of proton-proton collisions at $\sqrt{s} = 13$ TeV corresponding to an integrated luminosity of 137 fb^{-1} collected with the CMS detector in 2016–2018. No requirement is made on p_T^{miss} . The dominant $t\bar{t}$ background is predicted from data using a simultaneous fit of the jet multiplicity distribution across four bins of a neural network score.

The results are interpreted in terms of top squark pair production in the context of R -parity violating (RPV) and stealth supersymmetry models. Top squark masses ($m_{\tilde{t}}$) up to 670 GeV are excluded at 95% confidence level for the RPV model in which the top squark decays to a top quark

and the lightest neutralino, which subsequently decays to three light-flavor quarks via an off shell squark through a trilinear coupling λ'' . Top squark masses up to 870 GeV are excluded for the stealth supersymmetry model in which the top squark decays to a top quark, three gluons, and a gravitino via intermediate hidden sector particles. The maximum observed local significance is 2.8 standard deviations corresponding to a best fit signal strength of 0.21 ± 0.07 for the RPV model with $m_{\tilde{t}} = 400$ GeV.

ACKNOWLEDGMENTS

We congratulate our colleagues in the CERN accelerator departments for the excellent performance of the LHC and thank the technical and administrative staffs at CERN and at other CMS institutes for their contributions to the success of the CMS effort. In addition, we gratefully acknowledge the computing centers and personnel of the Worldwide LHC Computing Grid and other centers for delivering so effectively the computing infrastructure essential to our analyses. Finally, we acknowledge the enduring support for the construction and operation of the LHC, the CMS detector, and the supporting computing infrastructure provided by the following funding agencies: BMBWF and FWF (Austria); FNRS and FWO (Belgium); CNPq, CAPES, FAPERJ, FAPERGS, and FAPESP (Brazil); MES (Bulgaria); CERN; CAS, MoST, and NSFC (China); COLCIENCIAS (Colombia); MSES and CSF (Croatia); RIF (Cyprus); SENESCYT (Ecuador); MoER, ERC PUT and ERDF (Estonia); Academy of Finland, MEC, and HIP

(Finland); CEA and CNRS/IN2P3 (France); BMBF, DFG, and HGF (Germany); GSRT (Greece); NKFI (Hungary); DAE and DST (India); IPM (Iran); SFI (Ireland); INFN (Italy); MSIP and NRF (Republic of Korea); MES (Latvia); LAS (Lithuania); MOE and UM (Malaysia); BUAP, CINVESTAV, CONACYT, LNS, SEP, and UASLP-FAI (Mexico); MOS (Montenegro); MBIE (New Zealand); PAEC (Pakistan); MSHE and NSC (Poland); FCT (Portugal); JINR (Dubna); MON, RosAtom, RAS, RFBR, and NRC KI (Russia); MESTD (Serbia); SEIDI, CPAN, PCTI, and FEDER (Spain); MOSTR (Sri Lanka); Swiss Funding Agencies (Switzerland); MST (Taipei); ThEPCenter, IPST, STAR, and NSTDA (Thailand); TUBITAK and TAEK (Turkey); NASU (Ukraine); STFC (United Kingdom); DOE and NSF (USA). Individuals have received support from the Marie-Curie program and the European Research Council and Horizon 2020 Grant, Contracts No. 675440, No. 724704, No. 752730, and No. 765710 (European Union); the Leventis Foundation; the Alfred P. Sloan Foundation; the Alexander von Humboldt Foundation; the Belgian Federal Science Policy Office; the Fonds pour la Formation à la Recherche dans l'Industrie et dans l'Agriculture (FRIA-Belgium); the Agentschap voor Innovatie door Wetenschap en Technologie (IWT-Belgium); the F. R. S.-FNRS and FWO (Belgium) under the “Excellence of Science—EOS”—be.h Project No. 30820817; the Beijing Municipal Science and Technology Commission, No. Z191100007219010; the Ministry of Education, Youth and Sports (MEYS) of the Czech Republic; the Deutsche Forschungsgemeinschaft (DFG), under Germany’s Excellence Strategy—EXC

2121 “Quantum Universe”—390833306, and under Project No. 400140256—GRK2497; the Lendület (“Momentum”) Program and the János Bolyai Research Scholarship of the Hungarian Academy of Sciences, the New National Excellence Program ÚNKP, the NKFI Research Grants No. 123842, No. 123959, No. 124845, No. 124850, No. 125105, No. 128713, No. 128786, and No. 129058 (Hungary); the Council of Science and Industrial Research, India; the HOMING PLUS program of the Foundation for Polish Science, cofinanced from European Union, Regional Development Fund, the Mobility Plus program of the Ministry of Science and Higher Education, the National Science Center (Poland), Contracts Harmonia No. 2014/14/M/ST2/00428, Opus No. 2014/13/B/ST2/02543, No. 2014/15/B/ST2/03998, and No. 2015/19/B/ST2/02861, Sonata-bis No. 2012/07/E/ST2/01406; the National Priorities Research Program by Qatar National Research Fund; the Ministry of Science and Higher Education, Project No. 0723-2020-0041 (Russia); the Programa Estatal de Fomento de la Investigación Científica y Técnica de Excelencia María de Maeztu, Grant No. MDM-2015-0509 and the Programa Severo Ochoa del Principado de Asturias; the Thalís and Aristeia programs cofinanced by EU-ESF and the Greek NSRF; the Rachadapisek Sompot Fund for Postdoctoral Fellowship, Chulalongkorn University and the Chulalongkorn Academic into Its 2nd Century Project Advancement Project (Thailand); the Kavli Foundation; the Nvidia Corporation; the SuperMicro Corporation; the Welch Foundation, Contract No. C-1845; and the Weston Havens Foundation (USA).

-
- [1] P. Fayet and S. Ferrara, *Supersymmetry*, *Phys. Rep.* **32**, 249 (1977).
- [2] S. P. Martin, A supersymmetry primer, *Adv. Ser. Dir. High Energy Phys.* **21**, 1 (1997).
- [3] S. Dimopoulos and G. F. Giudice, Naturalness constraints in supersymmetric theories with nonuniversal soft terms, *Phys. Lett. B* **357**, 573 (1995).
- [4] R. Barbieri and G. F. Giudice, Upper bounds on supersymmetric particle masses, *Nucl. Phys.* **B306**, 63 (1988).
- [5] A. Pomarol and D. Tommasini, Horizontal symmetries for the supersymmetric flavor problem, *Nucl. Phys.* **B466**, 3 (1996).
- [6] A. G. Cohen, D. B. Kaplan, and A. E. Nelson, The more minimal supersymmetric standard model, *Phys. Lett. B* **388**, 588 (1996).
- [7] M. Papucci, J. T. Ruderman, and A. Weiler, Natural SUSY endures, *J. High Energy Phys.* **09** (2012) 035.
- [8] C. Brust, A. Katz, S. Lawrence, and R. Sundrum, SUSY, the third generation and the LHC, *J. High Energy Phys.* **03** (2012) 103.
- [9] R. Barbier, C. Berat, M. Besancon, M. Chemtob, A. Deandrea, E. Dudas, P. Fayet, S. Lavignac, G. Moreau, E. Perez, and Y. Sirois, *R*-parity violating supersymmetry, *Phys. Rep.* **420**, 1 (2005).
- [10] D. S. M. Alves, E. Izaguirre, and J. G. Wacker, Where the sidewalk ends: Jets and missing energy search strategies for the 7 TeV LHC, *J. High Energy Phys.* **10** (2011) 012.
- [11] M. Lisanti, P. Schuster, M. Strassler, and N. Toro, Study of LHC searches for a lepton and many jets, *J. High Energy Phys.* **11** (2012) 081.
- [12] J. Fan, M. Reece, and J. T. Ruderman, Stealth supersymmetry, *J. High Energy Phys.* **11** (2011) 012.
- [13] G. F. Giudice and R. Rattazzi, Theories with gauge mediated supersymmetry breaking, *Phys. Rep.* **322**, 419 (1999).
- [14] S. P. Martin, Compressed supersymmetry and natural neutralino dark matter from top squark-mediated annihilation to top quarks, *Phys. Rev. D* **75**, 115005 (2007).
- [15] T. J. LeCompte and S. P. Martin, Large hadron collider reach for supersymmetric models with compressed mass spectra, *Phys. Rev. D* **84**, 015004 (2011).

- [16] M. J. Strassler, Why unparticle models with mass gaps are examples of hidden valleys, [arXiv:0801.0629](https://arxiv.org/abs/0801.0629).
- [17] CMS Collaboration, Search for supersymmetry in proton-proton collisions at 13 TeV using identified top quarks, *Phys. Rev. D* **97**, 012007 (2018).
- [18] CMS Collaboration, Search for direct production of supersymmetric partners of the top quark in the all-jets final state in proton-proton collisions at $\sqrt{s} = 13$ TeV, *J. High Energy Phys.* **10** (2017) 005.
- [19] CMS Collaboration, Search for top squark pair production in pp collisions at $\sqrt{s} = 13$ TeV using single lepton events, *J. High Energy Phys.* **10** (2017) 019.
- [20] CMS Collaboration, Search for top squarks and dark matter particles, in opposite-charge dilepton final states at $\sqrt{s} = 13$ TeV, *Phys. Rev. D* **97**, 032009 (2018).
- [21] ATLAS Collaboration, Search for a scalar partner of the top quark in the jets plus missing transverse momentum final state at $\sqrt{s} = 13$ TeV with the ATLAS detector, *J. High Energy Phys.* **12** (2017) 085.
- [22] ATLAS Collaboration, Search for top-squark pair production in final states with one lepton, jets, and missing transverse momentum using 36 fb^{-1} of $\sqrt{s} = 13$ TeV pp collision data with the ATLAS detector, *J. High Energy Phys.* **06** (2018) 108.
- [23] J. Fan, M. Reece, and J. T. Ruderman, A stealth supersymmetry sampler, *J. High Energy Phys.* **07** (2012) 196.
- [24] J. Fan, R. Krall, D. Pinner, M. Reece, and J. T. Ruderman, Stealth supersymmetry simplified, *J. High Energy Phys.* **07** (2016) 016.
- [25] ATLAS Collaboration, A search for pair-produced resonances in four-jet final states at $\sqrt{s} = 13$ TeV with the ATLAS detector, *Eur. Phys. J. C* **78**, 250 (2018).
- [26] CMS Collaboration, Search for pair-produced resonances decaying to quark pairs in proton-proton collisions at $\sqrt{s} = 13$ TeV, *Phys. Rev. D* **98**, 112014 (2018).
- [27] ATLAS Collaboration, Search for B-L R -parity-violating top squarks in $\sqrt{s} = 13$ TeV pp collisions with the ATLAS experiment, *Phys. Rev. D* **97**, 032003 (2018).
- [28] CMS Collaboration, Search for pair production of third-generation scalar leptoquarks and top squarks in proton-proton collisions at $\sqrt{s} = 8$ TeV, *Phys. Lett. B* **739**, 229 (2014).
- [29] CMS Collaboration, Search for R -parity violating decays of a top squark in proton-proton collisions at $\sqrt{s} = 8$ TeV, *Phys. Lett. B* **760**, 178 (2016).
- [30] ATLAS Collaboration, Search for new phenomena in a lepton plus high jet multiplicity final state with the ATLAS experiment using $\sqrt{s} = 13$ TeV proton-proton collision data, *J. High Energy Phys.* **09** (2017) 088.
- [31] CMS Collaboration, Search for stealth supersymmetry in events with jets, either photons or leptons, and low missing transverse momentum in pp collisions at 8 TeV, *Phys. Lett. B* **743**, 503 (2015).
- [32] CMS Collaboration, Search for supersymmetry in events with photons and low missing transverse energy in pp collisions at $\sqrt{s} = 7$ TeV, *Phys. Lett. B* **719**, 42 (2013).
- [33] J. A. Evans and Y. Kats, LHC coverage of RPV MSSM with light stops, *J. High Energy Phys.* **04** (2013) 028.
- [34] CMS Collaboration, The CMS experiment at the CERN LHC, *J. Instrum.* **3**, S08004 (2008).
- [35] CMS Collaboration, The CMS trigger system, *J. Instrum.* **12**, P01020 (2017).
- [36] CMS Collaboration, Particle-flow reconstruction and global event description with the CMS detector, *J. Instrum.* **12**, P10003 (2017).
- [37] M. Cacciari, G. P. Salam, and G. Soyez, The anti- k_T jet clustering algorithm, *J. High Energy Phys.* **04** (2008) 063.
- [38] M. Cacciari, G. P. Salam, and G. Soyez, FastJet user manual, *Eur. Phys. J. C* **72**, 1896 (2012).
- [39] CMS Collaboration, Technical proposal for the phase-II upgrade of the compact Muon solenoid, CMS Technical Proposal CERN-LHCC-2015-010, CMS-TDR-15-02, CERN, 2015, <http://cds.cern.ch/record/2020886>.
- [40] CMS Collaboration, Performance of electron reconstruction and selection with the CMS detector in proton-proton collisions at $\sqrt{s} = 8$ TeV, *J. Instrum.* **10**, P06005 (2015).
- [41] CMS Collaboration, Performance of the CMS muon detector and muon reconstruction with proton-proton collisions at $\sqrt{s} = 13$ TeV, *J. Instrum.* **13**, P06015 (2018).
- [42] K. Rehermann and B. Tweedie, Efficient identification of boosted semileptonic top quarks at the LHC, *J. High Energy Phys.* **03** (2011) 059.
- [43] CMS Collaboration, Jet performance in pp collisions at 7 TeV, CMS Physics Analysis Summary CMS-PAS-JME-10-003 (2010), <https://cds.cern.ch/record/1279362>.
- [44] CMS Collaboration, Jet algorithms performance in 13 TeV data, CMS Physics Analysis Summary CMS-PAS-JME-16-003 (2017), <http://cds.cern.ch/record/2256875>.
- [45] CMS Collaboration, Jet energy scale and resolution in the CMS experiment in pp collisions at 8 TeV, *J. Instrum.* **12**, P02014 (2017).
- [46] CMS Collaboration, Jet energy scale and resolution performance with 13 TeV data collected by CMS in 2016–2018, CMS Detector Performance Note CMS-DP-2020-019, 2020, <https://cdsweb.cern.ch/record/2715872>.
- [47] M. Cacciari and G. P. Salam, Pileup subtraction using jet areas, *Phys. Lett. B* **659**, 119 (2008).
- [48] CMS Collaboration, Identification of heavy-flavour jets with the CMS detector in pp collisions at 13 TeV, *J. Instrum.* **13**, P05011 (2018).
- [49] P. Nason, A new method for combining NLO QCD with shower Monte Carlo algorithms, *J. High Energy Phys.* **11** (2004) 040.
- [50] S. Frixione, P. Nason, and C. Oleari, Matching NLO QCD computations with parton shower simulations: The POWHEG method, *J. High Energy Phys.* **11** (2007) 070.
- [51] S. Alioli, P. Nason, C. Oleari, and E. Re, A general framework for implementing NLO calculations in shower Monte Carlo programs: The POWHEG box, *J. High Energy Phys.* **06** (2010) 043.
- [52] S. Frixione, P. Nason, and G. Ridolfi, A positive-weight next-to-leading-order Monte Carlo for heavy flavour hadroproduction, *J. High Energy Phys.* **09** (2007) 126.
- [53] R. Frederix, E. Re, and P. Torrielli, Single-top t -channel hadroproduction in the four-flavour scheme with POWHEG and aMC@NLO, *J. High Energy Phys.* **09** (2012) 130.
- [54] J. Alwall, R. Frederix, S. Frixione, V. Hirschi, F. Maltoni, O. Mattelaer, H. S. Shao, T. Stelzer, P. Torrielli, and M. Zaro, The automated computation of tree-level and next-to-leading order differential cross sections, and their matching

- to parton shower simulations, *J. High Energy Phys.* **07** (2014) 079.
- [55] A. Kalogeropoulos and J. Alwall, The SysCalc code: A tool to derive theoretical systematic uncertainties, [arXiv:1801.08401](https://arxiv.org/abs/1801.08401).
- [56] T. Sjöstrand, S. Ask, J. R. Christiansen, R. Corke, N. Desai, P. Ilten, S. Mrenna, S. Prestel, C. O. Rasmussen, and P. Z. Skands, An introduction to PYTHIA 8.2, *Comput. Phys. Commun.* **191**, 159 (2015).
- [57] C. Borschensky, M. Krämer, A. Kulesza, M. Mangano, S. Padhi, T. Plehn, and X. Portell, Squark and gluino production cross sections in pp collisions at $\sqrt{s} = 13, 14, 33$ and 100 TeV, *Eur. Phys. J. C* **74**, 3174 (2014).
- [58] W. Beenakker, C. Borschensky, M. Krämer, A. Kulesza, and E. Laenen, NNLL-fast: Predictions for coloured supersymmetric particle production at the LHC with threshold and Coulomb resummation, *J. High Energy Phys.* **12** (2016) 133.
- [59] R. D. Ball *et al.* (NNPDF Collaboration), Parton distributions for the LHC Run II, *J. High Energy Phys.* **04** (2015) 040.
- [60] R. D. Ball *et al.* (NNPDF Collaboration), Parton distributions from high-precision collider data, *Eur. Phys. J. C* **77**, 663 (2017).
- [61] CMS Collaboration, Event generator tunes obtained from underlying event and multiparton scattering measurements, *Eur. Phys. J. C* **76**, 155 (2016).
- [62] CMS Collaboration, Investigations of the impact of the parton shower tuning in PYTHIA 8 in the modelling of $t\bar{t}$ at $\sqrt{s} = 8$ and 13 TeV, CMS Physics Analysis Summary CMS-PAS-TOP-16-021, 2016, <http://cds.cern.ch/record/2235192>.
- [63] CMS Collaboration, Extraction and validation of a new set of CMS PYTHIA 8 tunes from underlying-event measurements, *Eur. Phys. J. C* **80**, 4 (2020).
- [64] S. Agostinelli *et al.* (GEANT4 Collaboration), GEANT4—A simulation toolkit, *Nucl. Instrum. Methods Phys. Res., Sect. A* **506**, 250 (2003).
- [65] M. Czakon and A. Mitov, Top++: A program for the calculation of the top-pair cross-section at hadron colliders, *Comput. Phys. Commun.* **185**, 2930 (2014).
- [66] P. Kant, O. M. Kind, T. Kintscher, T. Lohse, T. Martini, S. Mölbitz, P. Rieck, and P. Uwer, HATHOR for single top-quark production: Updated predictions and uncertainty estimates for single top-quark production in hadronic collisions, *Comput. Phys. Commun.* **191**, 74 (2015).
- [67] M. Aliev, H. Lacker, U. Langenfeld, S. Moch, P. Uwer, and M. Wiedermann, HATHOR: HAdronic Top and Heavy quarks crOss section calculatoR, *Comput. Phys. Commun.* **182**, 1034 (2011).
- [68] T. Gehrmann, M. Grazzini, S. Kallweit, P. Maierhöfer, A. von Manteuffel, S. Pozzorini, D. Rathlev, and L. Tancredi, W^+W^- Production at Hadron Colliders in Next to Next to Leading Order QCD, *Phys. Rev. Lett.* **113**, 212001 (2014).
- [69] J. M. Campbell and R. K. Ellis, An update on vector boson pair production at hadron colliders, *Phys. Rev. D* **60**, 113006 (1999).
- [70] J. M. Campbell, R. K. Ellis, and C. Williams, Vector boson pair production at the LHC, *J. High Energy Phys.* **07** (2011) 018.
- [71] Y. Li and F. Petriello, Combining QCD and electroweak corrections to dilepton production in FEWZ, *Phys. Rev. D* **86**, 094034 (2012).
- [72] Y. Ganin and V. Lempitsky, Unsupervised domain adaptation by backpropagation, [arXiv:1409.7495](https://arxiv.org/abs/1409.7495).
- [73] G. C. Fox and S. Wolfram, Observables for the Analysis of Event Shapes in e^+e^- Annihilation and Other Processes, *Phys. Rev. Lett.* **41**, 1581 (1978).
- [74] J. D. Bjorken and S. J. Brodsky, Statistical model for electron-positron annihilation into hadrons, *Phys. Rev. D* **1**, 1416 (1970).
- [75] E. Gerwick, T. Plehn, S. Schumann, and P. Schichtel, Scaling patterns for QCD jets, *J. High Energy Phys.* **10** (2012) 162.
- [76] M. Cacciari, S. Frixione, M. L. Mangano, P. Nason, and G. Ridolfi, The $t\bar{t}$ cross-section at 1.8 TeV and 1.96 TeV: A study of the systematics due to parton densities and scale dependence, *J. High Energy Phys.* **04** (2004) 068.
- [77] S. Catani, D. de Florian, M. Grazzini, and P. Nason, Soft gluon resummation for Higgs boson production at hadron colliders, *J. High Energy Phys.* **07** (2003) 028.
- [78] CMS Collaboration, Measurement of the inelastic proton-proton cross section at $\sqrt{s} = 13$ TeV, *J. High Energy Phys.* **07** (2018) 161.
- [79] CMS Collaboration, CMS luminosity measurements for the 2016 data taking period, CMS Physics Analysis Summary, Technical Report No. CMS-PAS-LUM-17-001, 2017, <https://cds.cern.ch/record/2257069>.
- [80] CMS Collaboration, CMS luminosity measurements for the 2017 data taking period at $\sqrt{s} = 13$ TeV, CMS Physics Analysis Summary, Technical Report No. CMS-PAS-LUM-17-004, 2017, <https://cds.cern.ch/record/2621960>.
- [81] CMS Collaboration, CMS luminosity measurements for the 2018 data taking period at $\sqrt{s} = 13$ TeV, CMS Physics Analysis Summary, Technical Report No. CMS-PAS-LUM-18-002, 2018, <https://cds.cern.ch/record/2676164>.
- [82] L. Demortier, p -values and nuisance parameters, in *Statistical Issues for LHC Physics. Proceedings, Workshop, PHYSTAT-LHC, Geneva, Switzerland, 2007* (CERN, Geneva, 2008), p. 23, <http://dx.doi.org/10.5170/CERN-2008-001>.
- [83] ATLAS and CMS Collaborations, The LHC Higgs Combination Group, Procedure for the LHC Higgs boson search combination in Summer 2011, Technical Report No. CMS-NOTE-2011-005, ATL-PHYS-PUB-2011-11, 2011, <https://cds.cern.ch/record/1379837>.
- [84] T. Junk, Confidence level computation for combining searches with small statistics, *Nucl. Instrum. Methods Phys. Res., Sect. A* **434**, 435 (1999).
- [85] A. L. Read, Presentation of search results: The CL_s technique, *J. Phys. G* **28**, 2693 (2002).
- [86] G. Cowan, K. Cranmer, E. Gross, and O. Vitells, Asymptotic formulae for likelihood-based tests of new physics, *Eur. Phys. J. C* **71**, 1554 (2011); Erratum, *Eur. Phys. J. C* **73**, 2501 (2013).

A. M. Sirunyan,^{1,a} A. Tumasyan,¹ W. Adam,² J. W. Andrejkovic,² T. Bergauer,² S. Chatterjee,² M. Dragicevic,² A. Escalante Del Valle,² R. Frühwirth,^{2,b} M. Jeitler,^{2,b} N. Krammer,² L. Lechner,² D. Liko,² I. Mikulec,² F. M. Pitters,² J. Schieck,^{2,b} R. Schöfbeck,² M. Spanring,² S. Templ,² W. Waltenberger,² C.-E. Wulz,^{2,b} V. Chekhovsky,³ A. Litomin,³ V. Makarenko,³ M. R. Darwish,^{4,c} E. A. De Wolf,⁴ X. Janssen,⁴ T. Kello,^{4,d} A. Lelek,⁴ H. Rejeb Sfar,⁴ P. Van Mechelen,⁴ S. Van Putte,⁴ N. Van Remortel,⁴ F. Blekman,⁵ E. S. Bols,⁵ J. D'Hondt,⁵ J. De Clercq,⁵ M. Delcourt,⁵ S. Lowette,⁵ S. Moortgat,⁵ A. Morton,⁵ D. Müller,⁵ A. R. Sahasransu,⁵ S. Tavernier,⁵ W. Van Doninck,⁵ P. Van Mulders,⁵ D. Beghin,⁶ B. Bilin,⁶ B. Clerbaux,⁶ G. De Lentdecker,⁶ L. Favart,⁶ A. Grebenyuk,⁶ A. K. Kalsi,⁶ K. Lee,⁶ M. Mahdavihorrani,⁶ I. Makarenko,⁶ L. Moureaux,⁶ L. Pétré,⁶ A. Popov,⁶ N. Postiau,⁶ E. Starling,⁶ L. Thomas,⁶ M. Vanden Bemden,⁶ C. Vander Velde,⁶ P. Vanlaer,⁶ D. Vannerom,⁶ L. Wezenbeek,⁶ T. Cornelis,⁷ D. Dobur,⁷ M. Gruchala,⁷ G. Mestdach,⁷ M. Niedziela,⁷ C. Roskas,⁷ K. Skovpen,⁷ M. Tytgat,⁷ W. Verbeke,⁷ B. Vermassen,⁷ M. Vit,⁷ A. Bethani,⁸ G. Bruno,⁸ F. Bury,⁸ C. Caputo,⁸ P. David,⁸ C. Delaere,⁸ I. S. Donertas,⁸ A. Giammanco,⁸ V. Lemaître,⁸ K. Mondal,⁸ J. Prisciandaro,⁸ A. Taliercio,⁸ M. Teklishyn,⁸ P. Vischia,⁸ S. Wertz,⁸ S. Wuyckens,⁸ G. A. Alves,⁹ C. Hensel,⁹ A. Moraes,⁹ W. L. Aldá Júnior,¹⁰ M. Barroso Ferreira Filho,¹⁰ H. Brandao Malbousson,¹⁰ W. Carvalho,¹⁰ J. Chinellato,^{10,e} E. M. Da Costa,¹⁰ G. G. Da Silveira,^{10,f} D. De Jesus Damiao,¹⁰ S. Fonseca De Souza,¹⁰ D. Matos Figueiredo,¹⁰ C. Mora Herrera,¹⁰ K. Mota Amarilo,¹⁰ L. Mundim,¹⁰ H. Nogima,¹⁰ P. Rebello Teles,¹⁰ L. J. Sanchez Rosas,¹⁰ A. Santoro,¹⁰ S. M. Silva Do Amaral,¹⁰ A. Sznajder,¹⁰ M. Thiel,¹⁰ F. Torres Da Silva De Araujo,¹⁰ A. Vilela Pereira,¹⁰ C. A. Bernardes,^{11a} L. Calligaris,^{11a} T. R. Fernandez Perez Tomei,^{11a} E. M. Gregores,^{11a,11b} D. S. Lemos,^{11a} P. G. Mercadante,^{11a,11b} S. F. Novaes,^{11a} Sandra S. Padula,^{11a} A. Aleksandrov,¹² G. Antchev,¹² I. Atanasov,¹² R. Hadjiiska,¹² P. Iaydjiev,¹² M. Misheva,¹² M. Rodozov,¹² M. Shopova,¹² G. Sultanov,¹² A. Dimitrov,¹³ T. Ivanov,¹³ L. Litov,¹³ B. Pavlov,¹³ P. Petkov,¹³ A. Petrov,¹³ T. Cheng,¹⁴ W. Fang,^{14,d} Q. Guo,¹⁴ T. Javaid,^{14,g} M. Mittal,¹⁴ H. Wang,¹⁴ L. Yuan,¹⁴ M. Ahmad,¹⁵ G. Bauer,¹⁵ C. Dozen,^{15,h} Z. Hu,¹⁵ J. Martins,^{15,i} Y. Wang,¹⁵ K. Yi,^{15,j,k} E. Chapon,¹⁶ G. M. Chen,^{16,g} H. S. Chen,^{16,g} M. Chen,¹⁶ A. Kapoor,¹⁶ D. Leggat,¹⁶ H. Liao,¹⁶ Z.-A. LIU,^{16,l} R. Sharma,¹⁶ A. Spiezia,¹⁶ J. Tao,¹⁶ J. Thomas-Wilsker,¹⁶ J. Wang,¹⁶ H. Zhang,¹⁶ S. Zhang,^{16,g} J. Zhao,¹⁶ A. Agapitos,¹⁷ Y. Ban,¹⁷ C. Chen,¹⁷ Q. Huang,¹⁷ A. Levin,¹⁷ Q. Li,¹⁷ M. Lu,¹⁷ X. Lyu,¹⁷ Y. Mao,¹⁷ S. J. Qian,¹⁷ D. Wang,¹⁷ Q. Wang,¹⁷ J. Xiao,¹⁷ Z. You,¹⁸ X. Gao,^{19,d} H. Okawa,¹⁹ M. Xiao,²⁰ C. Avila,²¹ A. Cabrera,²¹ C. Florez,²¹ J. Fraga,²¹ A. Sarkar,²¹ M. A. Segura Delgado,²¹ J. Jaramillo,²² J. Mejia Guisao,²² F. Ramirez,²² J. D. Ruiz Alvarez,²² C. A. Salazar González,²² N. Vanegas Arbelaez,²² D. Giljanovic,²³ N. Godinovic,²³ D. Lelas,²³ I. Puljak,²³ Z. Antunovic,²⁴ M. Kovac,²⁴ T. Sculac,²⁴ V. Brigljevic,²⁵ D. Ferencek,²⁵ D. Majumder,²⁵ M. Roguljic,²⁵ A. Starodumov,^{25,m} T. Susa,²⁵ A. Attikis,²⁶ E. Erodoutou,²⁶ A. Ioannou,²⁶ G. Kole,²⁶ M. Kolosova,²⁶ S. Konstantinou,²⁶ J. Mousa,²⁶ C. Nicolaou,²⁶ F. Ptochos,²⁶ P. A. Razis,²⁶ H. Rykaczewski,²⁶ H. Saka,²⁶ M. Finger,^{27,n} M. Finger Jr.,^{27,n} A. Kveton,²⁷ E. Ayala,²⁸ E. Carrera Jarrin,²⁹ S. Abu Zeid,^{30,o} S. Khalil,^{30,p} E. Salama,^{30,q,o} A. Lotfy,³¹ Y. Mohammed,³¹ S. Bhowmik,³² A. Carvalho Antunes De Oliveira,³² R. K. Dewanjee,³² K. Ehataht,³² M. Kadastik,³² J. Pata,³² M. Raidal,³² C. Veelken,³² P. Eerola,³³ L. Forthomme,³³ H. Kirschenmann,³³ K. Osterberg,³³ M. Voutilainen,³³ E. Brücken,³⁴ F. Garcia,³⁴ J. Havukainen,³⁴ V. Karimäki,³⁴ M. S. Kim,³⁴ R. Kinnunen,³⁴ T. Lampén,³⁴ K. Lassila-Perini,³⁴ S. Lehti,³⁴ T. Lindén,³⁴ H. Siikonen,³⁴ E. Tuominen,³⁴ J. Tuominiemi,³⁴ P. Luukka,³⁵ H. Petrow,³⁵ T. Tuuva,³⁵ C. Amendola,³⁶ M. Besancon,³⁶ F. Couderc,³⁶ M. Dejardin,³⁶ D. Denegri,³⁶ J. L. Faure,³⁶ F. Ferri,³⁶ S. Ganjour,³⁶ A. Givernaud,³⁶ P. Gras,³⁶ G. Hamel de Monchenault,³⁶ P. Jarry,³⁶ B. Lenzi,³⁶ E. Locci,³⁶ J. Malcles,³⁶ J. Rander,³⁶ A. Rosowsky,³⁶ M. Ö. Sahin,³⁶ A. Savoy-Navarro,^{36,r} M. Titov,³⁶ G. B. Yu,³⁶ S. Ahuja,³⁷ F. Beaudette,³⁷ M. Bonanomi,³⁷ A. Buchot Perraguin,³⁷ P. Busson,³⁷ C. Charlot,³⁷ O. Davignon,³⁷ B. Diab,³⁷ G. Falmagne,³⁷ S. Ghosh,³⁷ R. Granier de Cassagnac,³⁷ A. Hakimi,³⁷ I. Kucher,³⁷ A. Lobanov,³⁷ M. Nguyen,³⁷ C. Ochando,³⁷ P. Paganini,³⁷ J. Rembser,³⁷ R. Salerno,³⁷ J. B. Sauvan,³⁷ Y. Sirois,³⁷ A. Zabi,³⁷ A. Zghiche,³⁷ J.-L. Agram,^{38,s} J. Andrea,³⁸ D. Apparú,³⁸ D. Bloch,³⁸ G. Bourgatte,³⁸ J.-M. Brom,³⁸ E. C. Chabert,³⁸ C. Collard,³⁸ D. Darej,³⁸ J.-C. Fontaine,^{38,s} U. Goerlach,³⁸ C. Grimault,³⁸ A.-C. Le Bihan,³⁸ P. Van Hove,³⁸ E. Asilar,³⁹ S. Beauceron,³⁹ C. Bernet,³⁹ G. Boudoul,³⁹ C. Camen,³⁹ A. Carle,³⁹ N. Chanon,³⁹ D. Contardo,³⁹ P. Depasse,³⁹ H. El Mamouni,³⁹ J. Fay,³⁹ S. Gascon,³⁹ M. Gouzevitch,³⁹ B. Ille,³⁹ Sa. Jain,³⁹ I. B. Laktineh,³⁹ H. Lattaüd,³⁹ A. Lesauvage,³⁹ M. Lethuillier,³⁹ L. Mirabito,³⁹ K. Shchablo,³⁹ L. Torterotot,³⁹ G. Touquet,³⁹ M. Vander Donckt,³⁹ S. Viret,³⁹ G. Adamov,⁴⁰ Z. Tsamalaidze,^{40,n} L. Feld,⁴¹ K. Klein,⁴¹ M. Lipinski,⁴¹ D. Meuser,⁴¹ A. Pauls,⁴¹ M. P. Rauch,⁴¹ J. Schulz,⁴¹ M. Teroerde,⁴¹ D. Eliseev,⁴² M. Erdmann,⁴² P. Fackeldey,⁴² B. Fischer,⁴² S. Ghosh,⁴² T. Hebbeker,⁴² K. Hoepfner,⁴² H. Keller,⁴² L. Mastrolorenzo,⁴² M. Merschmeyer,⁴² A. Meyer,⁴² G. Mocellin,⁴² S. Mondal,⁴² S. Mukherjee,⁴² D. Noll,⁴² A. Novak,⁴² T. Pook,⁴² A. Pozdnyakov,⁴² Y. Rath,⁴² H. Reithler,⁴² J. Roemer,⁴² A. Schmidt,⁴² S. C. Schuler,⁴² A. Sharma,⁴² S. Wiedenbeck,⁴² S. Zaleski,⁴² C. Dziwok,⁴³ G. Flügge,⁴³ W. Haj Ahmad,^{43,t}

O. Hlushchenko,⁴³ T. Kress,⁴³ A. Nowack,⁴³ C. Pistone,⁴³ O. Pooth,⁴³ D. Roy,⁴³ H. Sert,⁴³ A. Stahl,^{43,u} T. Ziemons,⁴³ H. Aarup Petersen,⁴⁴ M. Aldaya Martin,⁴⁴ P. Asmuss,⁴⁴ I. Babounikau,⁴⁴ S. Baxter,⁴⁴ O. Behnke,⁴⁴ A. Bermúdez Martínez,⁴⁴ A. A. Bin Anuar,⁴⁴ K. Borrás,^{44,v} V. Botta,⁴⁴ D. Brunner,⁴⁴ A. Campbell,⁴⁴ A. Cardini,⁴⁴ P. Connor,⁴⁴ S. Consuegra Rodríguez,⁴⁴ V. Danilov,⁴⁴ M. M. Defranchis,⁴⁴ L. Didukh,⁴⁴ D. Domínguez Damiani,⁴⁴ G. Eckerlin,⁴⁴ D. Eckstein,⁴⁴ L. I. Estevez Banos,⁴⁴ E. Gallo,^{44,w} A. Geiser,⁴⁴ A. Giraldi,⁴⁴ A. Grohsjean,⁴⁴ M. Guthoff,⁴⁴ A. Harb,⁴⁴ A. Jafari,^{44,x} N. Z. Jomhari,⁴⁴ H. Jung,⁴⁴ A. Kasem,^{44,v} M. Kasemann,⁴⁴ H. Kaveh,⁴⁴ C. Kleinwort,⁴⁴ J. Knolle,⁴⁴ D. Krücker,⁴⁴ W. Lange,⁴⁴ T. Lenz,⁴⁴ J. Lidrych,⁴⁴ K. Lipka,⁴⁴ W. Lohmann,^{44,y} T. Madlener,⁴⁴ R. Mankel,⁴⁴ I.-A. Melzer-Pellmann,⁴⁴ J. Metwally,⁴⁴ A. B. Meyer,⁴⁴ M. Meyer,⁴⁴ J. Mnich,⁴⁴ A. Mussgiller,⁴⁴ V. Myronenko,⁴⁴ Y. Otariid,⁴⁴ D. Pérez Adán,⁴⁴ S. K. Pflitsch,⁴⁴ D. Pitzl,⁴⁴ A. Raspereza,⁴⁴ A. Saggio,⁴⁴ A. Saibel,⁴⁴ M. Savitskiy,⁴⁴ V. Scheurer,⁴⁴ C. Schwanenberger,⁴⁴ A. Singh,⁴⁴ R. E. Sosa Ricardo,⁴⁴ N. Tonon,⁴⁴ O. Turkot,⁴⁴ A. Vagnerini,⁴⁴ M. Van De Klundert,⁴⁴ R. Walsh,⁴⁴ D. Walter,⁴⁴ Y. Wen,⁴⁴ K. Wichmann,⁴⁴ C. Wissing,⁴⁴ S. Wuchterl,⁴⁴ O. Zenaiev,⁴⁴ R. Zlebciak,⁴⁴ R. Aggleton,⁴⁵ S. Bein,⁴⁵ L. Benato,⁴⁵ A. Benecke,⁴⁵ K. De Leo,⁴⁵ T. Dreyer,⁴⁵ M. Eich,⁴⁵ F. Feindt,⁴⁵ A. Fröhlich,⁴⁵ C. Garbers,⁴⁵ E. Garutti,⁴⁵ P. Gunnellini,⁴⁵ J. Haller,⁴⁵ A. Hinzmann,⁴⁵ A. Karavdina,⁴⁵ G. Kasieczka,⁴⁵ R. Klanner,⁴⁵ R. Kogler,⁴⁵ V. Kutzner,⁴⁵ J. Lange,⁴⁵ T. Lange,⁴⁵ A. Malara,⁴⁵ A. Nigamova,⁴⁵ K. J. Pena Rodriguez,⁴⁵ O. Rieger,⁴⁵ P. Schleper,⁴⁵ M. Schröder,⁴⁵ J. Schwandt,⁴⁵ D. Schwarz,⁴⁵ J. Sonneveld,⁴⁵ H. Stadie,⁴⁵ G. Steinbrück,⁴⁵ A. Tews,⁴⁵ B. Vormwald,⁴⁵ I. Zoi,⁴⁵ J. Bechtel,⁴⁶ T. Berger,⁴⁶ E. Butz,⁴⁶ R. Caspart,⁴⁶ T. Chwalek,⁴⁶ W. De Boer,⁴⁶ A. Dierlamm,⁴⁶ A. Droll,⁴⁶ K. El Morabit,⁴⁶ N. Faltermann,⁴⁶ K. Flöh,⁴⁶ M. Giffels,⁴⁶ J. o. Gosewisch,⁴⁶ A. Gottmann,⁴⁶ F. Hartmann,^{46,u} C. Heidecker,⁴⁶ U. Husemann,⁴⁶ I. Katkov,^{46,z} P. Keicher,⁴⁶ R. Koppenhöfer,⁴⁶ S. Maier,⁴⁶ M. Metzler,⁴⁶ S. Mitra,⁴⁶ Th. Müller,⁴⁶ M. Musich,⁴⁶ M. Neukum,⁴⁶ G. Quast,⁴⁶ K. Rabbertz,⁴⁶ J. Rauser,⁴⁶ D. Savoie,⁴⁶ D. Schäfer,⁴⁶ M. Schnepf,⁴⁶ D. Seith,⁴⁶ I. Shvetsov,⁴⁶ H. J. Simonis,⁴⁶ R. Ulrich,⁴⁶ J. Van Der Linden,⁴⁶ R. F. Von Cube,⁴⁶ M. Wassmer,⁴⁶ M. Weber,⁴⁶ S. Wieland,⁴⁶ R. Wolf,⁴⁶ S. Wozniewski,⁴⁶ S. Wunsch,⁴⁶ G. Anagnostou,⁴⁷ P. Asenov,⁴⁷ G. Daskalakis,⁴⁷ T. Geralis,⁴⁷ A. Kyriakis,⁴⁷ D. Loukas,⁴⁷ A. Stakia,⁴⁷ M. Diamantopoulou,⁴⁸ D. Karasavvas,⁴⁸ G. Karathanasis,⁴⁸ P. Kontaxakis,⁴⁸ C. K. Koraka,⁴⁸ A. Manousakis-Katsikakis,⁴⁸ A. Panagiotou,⁴⁸ I. Papavergou,⁴⁸ N. Saoulidou,⁴⁸ K. Theofilatos,⁴⁸ E. Tziaferi,⁴⁸ K. Vellidis,⁴⁸ E. Vourliotis,⁴⁸ G. Bakas,⁴⁹ K. Kousouris,⁴⁹ I. Papakrivopoulos,⁴⁹ G. Tsiopolitis,⁴⁹ A. Zacharopoulou,⁴⁹ I. Evangelou,⁵⁰ C. Foudas,⁵⁰ P. Gianneios,⁵⁰ P. Katsoulis,⁵⁰ P. Kokkas,⁵⁰ N. Manthos,⁵⁰ I. Papadopoulos,⁵⁰ J. Stroligas,⁵⁰ M. Csanad,⁵¹ M. M. A. Gadallah,^{51,aa} S. Lökös,^{51,bb} P. Major,⁵¹ K. Mandal,⁵¹ A. Mehta,⁵¹ G. Pasztor,⁵¹ A. J. Rád, ⁵¹ O. Surányi,⁵¹ G. I. Veres,⁵¹ M. Bartók,^{52,cc} G. Bencze,⁵² C. Hajdu,⁵² D. Horvath,^{52,dd} F. Sikler,⁵² V. Veszpremi,⁵² G. Vesztergombi,^{52,eee} S. Czellar,⁵³ J. Karancsi,^{53,cc} J. Molnar,⁵³ Z. Szillasi,⁵³ D. Teyssier,⁵³ P. Raics,⁵⁴ Z. L. Trocsanyi,^{54,ee} B. Ujvari,⁵⁴ T. Csorgo,^{55,ff} F. Nemes,^{55,ff} T. Novak,⁵⁵ S. Choudhury,⁵⁶ J. R. Komaragiri,⁵⁶ D. Kumar,⁵⁶ L. Panwar,⁵⁶ P. C. Tiwari,⁵⁶ S. Bahinipati,^{57,gg} D. Dash,⁵⁷ C. Kar,⁵⁷ P. Mal,⁵⁷ T. Mishra,⁵⁷ V. K. Muraleedharan Nair Bindhu,^{57,hh} A. Nayak,^{57,hh} P. Saha,⁵⁷ N. Sur,⁵⁷ S. K. Swain,⁵⁷ S. Bansal,⁵⁸ S. B. Beri,⁵⁸ V. Bhatnagar,⁵⁸ G. Chaudhary,⁵⁸ S. Chauhan,⁵⁸ N. Dhingra,^{58,ii} R. Gupta,⁵⁸ A. Kaur,⁵⁸ S. Kaur,⁵⁸ P. Kumari,⁵⁸ M. Meena,⁵⁸ K. Sandeep,⁵⁸ J. B. Singh,⁵⁸ A. K. Viridi,⁵⁸ A. Ahmed,⁵⁹ A. Bhardwaj,⁵⁹ B. C. Choudhary,⁵⁹ R. B. Garg,⁵⁹ M. Gola,⁵⁹ S. Keshri,⁵⁹ A. Kumar,⁵⁹ M. Naimuddin,⁵⁹ P. Priyanka,⁵⁹ K. Ranjan,⁵⁹ A. Shah,⁵⁹ M. Bharti,^{60,ij} R. Bhattacharya,⁶⁰ S. Bhattacharya,⁶⁰ D. Bhowmik,⁶⁰ S. Dutta,⁶⁰ B. Gomber,^{60,kk} M. Maity,^{60,ll} S. Nandan,⁶⁰ P. Palit,⁶⁰ P. K. Rout,⁶⁰ G. Saha,⁶⁰ B. Sahu,⁶⁰ S. Sarkar,⁶⁰ M. Sharan,⁶⁰ B. Singh,^{60,ji} S. Thakur,^{60,ji} P. K. Behera,⁶¹ S. C. Behera,⁶¹ P. Kalbhor,⁶¹ A. Muhammad,⁶¹ R. Pradhan,⁶¹ P. R. Pujahari,⁶¹ A. Sharma,⁶¹ A. K. Sikdar,⁶¹ D. Dutta,⁶² V. Jha,⁶² V. Kumar,⁶² D. K. Mishra,⁶² K. Naskar,^{62,mm} P. K. Netrakanti,⁶² L. M. Pant,⁶² P. Shukla,⁶² T. Aziz,⁶³ S. Dugad,⁶³ G. B. Mohanty,⁶³ U. Sarkar,⁶³ S. Banerjee,⁶⁴ S. Bhattacharya,⁶⁴ R. Chudasama,⁶⁴ M. Guchait,⁶⁴ S. Karmakar,⁶⁴ S. Kumar,⁶⁴ G. Majumder,⁶⁴ K. Mazumdar,⁶⁴ S. Mukherjee,⁶⁴ D. Roy,⁶⁴ S. Dube,⁶⁵ B. Kansal,⁶⁵ S. Pandey,⁶⁵ A. Rane,⁶⁵ A. Rastogi,⁶⁵ S. Sharma,⁶⁵ H. Bakhshiansohi,^{66,nn} M. Zeinali,^{66,oo} S. Chenarani,^{67,pp} S. M. Etesami,⁶⁷ M. Khakzad,⁶⁷ M. Mohammadi Najafabadi,⁶⁷ M. Felcini,⁶⁸ M. Grunewald,⁶⁸ M. Abbrescia,^{69a,69b} R. Aly,^{69a,69b,qq} C. Aruta,^{69a,69b} A. Colaleo,^{69a} D. Creanza,^{69a,69c} N. De Filippis,^{69a,69c} M. De Palma,^{69a,69b} A. Di Florio,^{69a,69b} A. Di Pilato,^{69a,69b} W. Elmetenawee,^{69a,69b} L. Fiore,^{69a} A. Gelmi,^{69a,69b} M. Gul,^{69a} G. Iaselli,^{69a,69c} M. Ince,^{69a,69b} S. Lezki,^{69a,69b} G. Maggi,^{69a,69c} M. Maggi,^{69a} I. Margjeka,^{69a,69b} V. Mastrapasqua,^{69a,69b} J. A. Merlin,^{69a} S. My,^{69a,69b} S. Nuzzo,^{69a,69b} A. Pompili,^{69a,69b} G. Pugliese,^{69a,69c} A. Ranieri,^{69a} G. Selvaggi,^{69a,69b} L. Silvestris,^{69a} F. M. Simone,^{69a,69b} R. Venditti,^{69a} P. Verwilligen,^{69a} G. Abbiendi,^{70a} C. Battilana,^{70a,70b} D. Bonacorsi,^{70a,70b} L. Borgonovi,^{70a} S. Braibant-Giacomelli,^{70a,70b} L. Brigliadori,^{70a} R. Campanini,^{70a,70b} P. Capiluppi,^{70a,70b} A. Castro,^{70a,70b} F. R. Cavallo,^{70a} C. Ciocca,^{70a} M. Cuffiani,^{70a,70b} G. M. Dallavalle,^{70a} T. Diotallevi,^{70a,70b} F. Fabbri,^{70a} A. Fanfani,^{70a,70b} E. Fontanesi,^{70a,70b} P. Giacomelli,^{70a} L. Giommi,^{70a,70b} C. Grandi,^{70a} L. Guiducci,^{70a,70b} F. Iemmi,^{70a,70b}

S. Lo Meo,^{70a,rr} S. Marcellini,^{70a} G. Masetti,^{70a} F. L. Navarria,^{70a,70b} A. Perrotta,^{70a} F. Primavera,^{70a,70b} A. M. Rossi,^{70a,70b}
 T. Rovelli,^{70a,70b} G. P. Siroli,^{70a,70b} N. Tosi,^{70a} S. Albergo,^{71a,71b,ss} S. Costa,^{71a,71b,ss} A. Di Mattia,^{71a} R. Potenza,^{71a,71b}
 A. Tricomi,^{71a,71b,ss} C. Tuve,^{71a,71b} G. Barbagli,^{72a} A. Cassese,^{72a} R. Ceccarelli,^{72a,72b} V. Ciulli,^{72a,72b} C. Civinini,^{72a}
 R. D'Alessandro,^{72a,72b} F. Fiori,^{72a,72b} E. Focardi,^{72a,72b} G. Latino,^{72a,72b} P. Lenzi,^{72a,72b} M. Lizzo,^{72a,72b} M. Meschini,^{72a}
 S. Paoletti,^{72a} R. Seidita,^{72a,72b} G. Sguazzoni,^{72a} L. Viliani,^{72a} L. Benussi,⁷³ S. Bianco,⁷³ D. Piccolo,⁷³ M. Bozzo,^{74a,74b}
 F. Ferro,^{74a} R. Mulargia,^{74a,74b} E. Robutti,^{74a} S. Tosi,^{74a,74b} A. Benaglia,^{75a} F. Brivio,^{75a,75b} F. Cetorelli,^{75a,75b}
 V. Ciriolo,^{75a,75b,u} F. De Guio,^{75a,75b} M. E. Dinardo,^{75a,75b} P. Dini,^{75a} S. Gennai,^{75a} A. Ghezzi,^{75a,75b} P. Govoni,^{75a,75b}
 L. Guzzi,^{75a,75b} M. Malberti,^{75a} S. Malvezzi,^{75a} A. Massironi,^{75a} D. Menasce,^{75a} F. Monti,^{75a,75b} L. Moroni,^{75a}
 M. Paganoni,^{75a,75b} D. Pedrini,^{75a} S. Ragazzi,^{75a,75b} T. Tabarelli de Fatis,^{75a,75b} D. Valsecchi,^{75a,75b,u} D. Zuolo,^{75a,75b}
 S. Buontempo,^{76a} F. Carnevali,^{76a,76b} N. Cavallo,^{76a,76c} A. De Iorio,^{76a,76b} F. Fabozzi,^{76a,76c} A. O. M. Iorio,^{76a,76b}
 L. Lista,^{76a,76b} S. Meola,^{76a,76d,u} P. Paolucci,^{76a,u} B. Rossi,^{76a} C. Sciacca,^{76a,76b} P. Azzi,^{77a} N. Bacchetta,^{77a} D. Bisello,^{77a,77b}
 P. Bortignon,^{77a} A. Bragagnolo,^{77a,77b} R. Carlin,^{77a,77b} P. Checchia,^{77a} P. De Castro Manzano,^{77a} T. Dorigo,^{77a}
 F. Gasparini,^{77a,77b} U. Gasparini,^{77a,77b} S. Y. Hoh,^{77a,77b} L. Layer,^{77a,tt} M. Margoni,^{77a,77b} A. T. Meneguzzo,^{77a,77b}
 M. Presilla,^{77a,77b} P. Ronchese,^{77a,77b} R. Rossin,^{77a,77b} F. Simonetto,^{77a,77b} G. Strong,^{77a} M. Tosi,^{77a,77b} H. YARAR,^{77a,77b}
 M. Zanetti,^{77a,77b} P. Zotto,^{77a,77b} A. Zucchetta,^{77a,77b} G. Zumerle,^{77a,77b} C. Aime,^{78a,78b} A. Braghieri,^{78a} S. Calzaferri,^{78a,78b}
 D. Fiorina,^{78a,78b} P. Montagna,^{78a,78b} S. P. Ratti,^{78a,78b} V. Re,^{78a} M. Ressegotti,^{78a,78b} C. Riccardi,^{78a,78b} P. Salvini,^{78a} I. Vai,^{78a}
 P. Vitulo,^{78a,78b} G. M. Bilei,^{79a} D. Ciangottini,^{79a,79b} L. Fanò,^{79a,79b} P. Lariccia,^{79a,79b} G. Mantovani,^{79a,79b} V. Mariani,^{79a,79b}
 M. Menichelli,^{79a} F. Moscatelli,^{79a} A. Piccinelli,^{79a,79b} A. Rossi,^{79a,79b} A. Santocchia,^{79a,79b} D. Spiga,^{79a} T. Tedeschi,^{79a,79b}
 P. Azzurri,^{80a} G. Bagliesi,^{80a} V. Bertacchi,^{80a,80c} L. Bianchini,^{80a} T. Boccali,^{80a} E. Bossini,^{80a} R. Castaldi,^{80a}
 M. A. Ciocci,^{80a,80b} R. Dell'Orso,^{80a} M. R. Di Domenico,^{80a,80d} S. Donato,^{80a} A. Giassi,^{80a} M. T. Grippo,^{80a} F. Ligabue,^{80a,80c}
 E. Manca,^{80a,80c} G. Mandorli,^{80a,80c} A. Messineo,^{80a,80b} F. Palla,^{80a} G. Ramirez-Sanchez,^{80a,80c} A. Rizzi,^{80a,80b}
 G. Rolandi,^{80a,80c} S. Roy Chowdhury,^{80a,80c} A. Scribano,^{80a} N. Shafiei,^{80a,80b} P. Spagnolo,^{80a} R. Tenchini,^{80a} G. Tonelli,^{80a,80b}
 N. Turini,^{80a,80d} A. Venturi,^{80a} P. G. Verdini,^{80a} F. Cavallari,^{81a} M. Cipriani,^{81a,81b} D. Del Re,^{81a,81b} E. Di Marco,^{81a}
 M. Diemoz,^{81a} E. Longo,^{81a,81b} P. Meridiani,^{81a} G. Organtini,^{81a,81b} F. Pandolfi,^{81a} R. Paramatti,^{81a,81b} C. Quaranta,^{81a,81b}
 S. Rahatlou,^{81a,81b} C. Rovelli,^{81a} F. Santanastasio,^{81a,81b} L. Soffi,^{81a,81b} R. Tramontano,^{81a,81b} N. Amapane,^{82a,82b}
 R. Arcidiacono,^{82a,82c} S. Argiro,^{82a,82b} M. Arneodo,^{82a,82c} N. Bartosik,^{82a} R. Bellan,^{82a,82b} A. Bellora,^{82a,82b}
 J. Berenguer Antequera,^{82a,82b} C. Biino,^{82a} A. Cappati,^{82a,82b} N. Cartiglia,^{82a} S. Cometti,^{82a} M. Costa,^{82a,82b}
 R. Covarelli,^{82a,82b} N. Demaria,^{82a} B. Kiani,^{82a,82b} F. Legger,^{82a} C. Mariotti,^{82a} S. Maselli,^{82a} E. Migliore,^{82a,82b}
 V. Monaco,^{82a,82b} E. Monteil,^{82a,82b} M. Monteno,^{82a} M. M. Obertino,^{82a,82b} G. Ortona,^{82a} L. Pacher,^{82a,82b} N. Pastrone,^{82a}
 M. Pelliccioni,^{82a} G. L. Pinna Angioni,^{82a,82b} M. Ruspa,^{82a,82c} R. Salvatico,^{82a,82b} K. Shchelina,^{82a,82b} F. Siviero,^{82a,82b}
 V. Sola,^{82a} A. Solano,^{82a,82b} D. Soldi,^{82a,82b} A. Staiano,^{82a} M. Tornago,^{82a,82b} D. Trocino,^{82a,82b} S. Belforte,^{83a}
 V. Candellise,^{83a,83b} M. Casarsa,^{83a} F. Cossutti,^{83a} A. Da Rold,^{83a,83b} G. Della Ricca,^{83a,83b} F. Vazzoler,^{83a,83b} S. Dogra,⁸⁴
 C. Huh,⁸⁴ B. Kim,⁸⁴ D. H. Kim,⁸⁴ G. N. Kim,⁸⁴ J. Lee,⁸⁴ S. W. Lee,⁸⁴ C. S. Moon,⁸⁴ Y. D. Oh,⁸⁴ S. I. Pak,⁸⁴
 B. C. Radburn-Smith,⁸⁴ S. Sekmen,⁸⁴ Y. C. Yang,⁸⁴ H. Kim,⁸⁵ D. H. Moon,⁸⁵ T. J. Kim,⁸⁶ J. Park,⁸⁶ S. Cho,⁸⁷ S. Choi,⁸⁷
 Y. Go,⁸⁷ B. Hong,⁸⁷ K. Lee,⁸⁷ K. S. Lee,⁸⁷ J. Lim,⁸⁷ J. Park,⁸⁷ S. K. Park,⁸⁷ J. Yoo,⁸⁷ J. Goh,⁸⁸ A. Gurtu,⁸⁸ H. S. Kim,⁸⁹
 Y. Kim,⁸⁹ J. Almond,⁹⁰ J. H. Bhyun,⁹⁰ J. Choi,⁹⁰ S. Jeon,⁹⁰ J. Kim,⁹⁰ J. S. Kim,⁹⁰ S. Ko,⁹⁰ H. Kwon,⁹⁰ H. Lee,⁹⁰ S. Lee,⁹⁰
 B. H. Oh,⁹⁰ M. Oh,⁹⁰ S. B. Oh,⁹⁰ H. Seo,⁹⁰ U. K. Yang,⁹⁰ I. Yoon,⁹⁰ D. Jeon,⁹¹ J. H. Kim,⁹¹ B. Ko,⁹¹ J. S. H. Lee,⁹¹
 I. C. Park,⁹¹ Y. Roh,⁹¹ D. Song,⁹¹ I. J. Watson,⁹¹ S. Ha,⁹² H. D. Yoo,⁹² Y. Choi,⁹³ Y. Jeong,⁹³ H. Lee,⁹³ Y. Lee,⁹³ I. Yu,⁹³
 T. Beyrouthy,⁹⁴ Y. Maghrbi,⁹⁴ V. Veckalns,^{95,uu} M. Ambrozas,⁹⁶ A. Juodagalvis,⁹⁶ A. Rinkevicius,⁹⁶ G. Tamulaitis,⁹⁶
 A. Vaitkevicius,⁹⁶ W. A. T. Wan Abdullah,⁹⁷ M. N. Yusli,⁹⁷ Z. Zolkapli,⁹⁷ J. F. Benitez,⁹⁸ A. Castaneda Hernandez,⁹⁸
 J. A. Murillo Quijada,⁹⁸ L. Valencia Palomo,⁹⁸ G. Ayala,⁹⁹ H. Castilla-Valdez,⁹⁹ E. De La Cruz-Burelo,⁹⁹
 I. Heredia-De La Cruz,^{99,vv} R. Lopez-Fernandez,⁹⁹ C. A. Mondragon Herrera,⁹⁹ D. A. Perez Navarro,⁹⁹
 A. Sanchez-Hernandez,⁹⁹ S. Carrillo Moreno,¹⁰⁰ C. Oropeza Barrera,¹⁰⁰ M. Ramirez-Garcia,¹⁰⁰ F. Vazquez Valencia,¹⁰⁰
 I. Pedraza,¹⁰¹ H. A. Salazar Ibarguen,¹⁰¹ C. Uribe Estrada,¹⁰¹ J. Mijuskovic,^{102,ww} N. Raicevic,¹⁰² D. Krofcheck,¹⁰³
 S. Bheesette,¹⁰⁴ P. H. Butler,¹⁰⁴ A. Ahmad,¹⁰⁵ M. I. Asghar,¹⁰⁵ A. Awais,¹⁰⁵ M. I. M. Awan,¹⁰⁵ H. R. Hoorani,¹⁰⁵
 W. A. Khan,¹⁰⁵ M. A. Shah,¹⁰⁵ M. Shoaib,¹⁰⁵ M. Waqas,¹⁰⁵ V. Avati,¹⁰⁶ L. Grzanka,¹⁰⁶ M. Malawski,¹⁰⁶ H. Bialkowska,¹⁰⁷
 M. Bluj,¹⁰⁷ B. Boimska,¹⁰⁷ T. Frueboes,¹⁰⁷ M. Górski,¹⁰⁷ M. Kazana,¹⁰⁷ M. Szeleper,¹⁰⁷ P. Traczyk,¹⁰⁷ P. Zalewski,¹⁰⁷
 K. Bunkowski,¹⁰⁸ K. Doroba,¹⁰⁸ A. Kalinowski,¹⁰⁸ M. Konecki,¹⁰⁸ J. Krolikowski,¹⁰⁸ M. Walczak,¹⁰⁸ M. Araujo,¹⁰⁹
 P. Bargassa,¹⁰⁹ D. Bastos,¹⁰⁹ A. Boletti,¹⁰⁹ P. Faccioli,¹⁰⁹ M. Gallinaro,¹⁰⁹ J. Hollar,¹⁰⁹ N. Leonardo,¹⁰⁹ T. Niknejad,¹⁰⁹

J. Seixas,¹⁰⁹ O. Toldaiev,¹⁰⁹ J. Varela,¹⁰⁹ S. Afanasiev,¹¹⁰ D. Budkouski,¹¹⁰ P. Bunin,¹¹⁰ M. Gavrilenko,¹¹⁰ I. Golutvin,¹¹⁰ I. Gorbunov,¹¹⁰ A. Kamenev,¹¹⁰ V. Karjavine,¹¹⁰ A. Lanev,¹¹⁰ A. Malakhov,¹¹⁰ V. Matveev,^{110,xx,yy} V. Palichik,¹¹⁰ V. Perelygin,¹¹⁰ M. Savina,¹¹⁰ D. Seitova,¹¹⁰ V. Shalaev,¹¹⁰ S. Shmatov,¹¹⁰ S. Shulha,¹¹⁰ V. Smirnov,¹¹⁰ O. Teryaev,¹¹⁰ N. Voytishin,¹¹⁰ A. Zarubin,¹¹⁰ I. Zhizhin,¹¹⁰ G. Gavrillov,¹¹¹ V. Golovtsov,¹¹¹ Y. Ivanov,¹¹¹ V. Kim,^{111,zz} E. Kuznetsova,^{111,aaa} V. Murzin,¹¹¹ V. Oreshkin,¹¹¹ I. Smirnov,¹¹¹ D. Sosnov,¹¹¹ V. Sulimov,¹¹¹ L. Uvarov,¹¹¹ S. Volkov,¹¹¹ A. Vorobyev,¹¹¹ Yu. Andreev,¹¹² A. Dermenev,¹¹² S. Gninenko,¹¹² N. Golubev,¹¹² A. Karneyeu,¹¹² M. Kirsanov,¹¹² N. Krasnikov,¹¹² A. Pashenkov,¹¹² G. Pivovarov,¹¹² D. Tlisov,^{112,a} A. Toropin,¹¹² V. Epshteyn,¹¹³ V. Gavrillov,¹¹³ N. Lychkovskaya,¹¹³ A. Nikitenko,^{113,bbb} V. Popov,¹¹³ G. Safronov,¹¹³ A. Spiridonov,¹¹³ A. Stepennov,¹¹³ M. Toms,¹¹³ E. Vlasov,¹¹³ A. Zhokin,¹¹³ T. Aushev,¹¹⁴ R. Chistov,^{115,ccc} M. Danilov,^{115,ddd} A. Oskin,¹¹⁵ P. Parygin,¹¹⁵ S. Polikarpov,^{115,ccc} V. Andreev,¹¹⁶ M. Azarkin,¹¹⁶ I. Dremin,¹¹⁶ M. Kirakosyan,¹¹⁶ A. Terkulov,¹¹⁶ A. Belyaev,¹¹⁷ E. Boos,¹¹⁷ M. Dubinin,^{117,eee} L. Dudko,¹¹⁷ A. Ershov,¹¹⁷ A. Gribushin,¹¹⁷ V. Klyukhin,¹¹⁷ O. Kodolova,¹¹⁷ I. Lokhtin,¹¹⁷ S. Obraztsov,¹¹⁷ S. Petrushanko,¹¹⁷ V. Savrin,¹¹⁷ A. Snigirev,¹¹⁷ V. Blinov,^{118,fff} T. Dimova,^{118,fff} L. Kardapoltsev,^{118,fff} I. Ovtin,^{118,fff} Y. Skovpen,^{118,fff} I. Azhgirey,¹¹⁹ I. Bayshev,¹¹⁹ V. Kachanov,¹¹⁹ A. Kalinin,¹¹⁹ D. Konstantinov,¹¹⁹ V. Petrov,¹¹⁹ R. Ryutin,¹¹⁹ A. Sobol,¹¹⁹ S. Troshin,¹¹⁹ N. Tyurin,¹¹⁹ A. Uzunian,¹¹⁹ A. Volkov,¹¹⁹ A. Babaev,¹²⁰ V. Okhotnikov,¹²⁰ L. Sukhikh,¹²⁰ V. Borchsh,¹²¹ V. Ivanchenko,¹²¹ E. Tcherniaev,¹²¹ P. Adzic,^{122,ggg} M. Dordevic,¹²² P. Milenovic,¹²² J. Milosevic,¹²² V. Milosevic,¹²² M. Aguilar-Benitez,¹²³ J. Alcaraz Maestre,¹²³ A. Álvarez Fernández,¹²³ I. Bachiller,¹²³ M. Barrio Luna,¹²³ Cristina F. Bedoya,¹²³ C. A. Carrillo Montoya,¹²³ M. Cepeda,¹²³ M. Cerrada,¹²³ N. Colino,¹²³ B. De La Cruz,¹²³ A. Delgado Peris,¹²³ J. P. Fernández Ramos,¹²³ J. Flix,¹²³ M. C. Fouz,¹²³ O. Gonzalez Lopez,¹²³ S. Goy Lopez,¹²³ J. M. Hernandez,¹²³ M. I. Josa,¹²³ J. León Holgado,¹²³ D. Moran,¹²³ Á. Navarro Tobar,¹²³ A. Pérez-Calero Yzquierdo,¹²³ J. Puerta Pelayo,¹²³ I. Redondo,¹²³ L. Romero,¹²³ S. Sánchez Navas,¹²³ M. S. Soares,¹²³ L. Urda Gómez,¹²³ C. Willmott,¹²³ J. F. de Trocóniz,¹²⁴ R. Reyes-Almanza,¹²⁴ B. Alvarez Gonzalez,¹²⁵ J. Cuevas,¹²⁵ C. Erice,¹²⁵ J. Fernandez Menendez,¹²⁵ S. Folgueras,¹²⁵ I. Gonzalez Caballero,¹²⁵ E. Palencia Cortezon,¹²⁵ C. Ramón Álvarez,¹²⁵ J. Ripoll Sau,¹²⁵ V. Rodríguez Bouza,¹²⁵ A. Trapote,¹²⁵ J. A. Brochero Cifuentes,¹²⁶ I. J. Cabrillo,¹²⁶ A. Calderon,¹²⁶ B. Chazin Quero,¹²⁶ J. Duarte Campderros,¹²⁶ M. Fernandez,¹²⁶ C. Fernandez Madrazo,¹²⁶ P. J. Fernández Manteca,¹²⁶ A. García Alonso,¹²⁶ G. Gomez,¹²⁶ C. Martinez Rivero,¹²⁶ P. Martinez Ruiz del Arbol,¹²⁶ F. Matorras,¹²⁶ J. Piedra Gomez,¹²⁶ C. Prieels,¹²⁶ F. Ricci-Tam,¹²⁶ T. Rodrigo,¹²⁶ A. Ruiz-Jimeno,¹²⁶ L. Scodellaro,¹²⁶ N. Trevisani,¹²⁶ I. Vila,¹²⁶ J. M. Vizan Garcia,¹²⁶ MK Jayananda,¹²⁷ B. Kailasapathy,^{127,hhh} D. U. J. Sonnadara,¹²⁷ DDC Wickramaratna,¹²⁷ W. G. D. Dharmaratna,¹²⁸ K. Liyanage,¹²⁸ N. Perera,¹²⁸ N. Wickramage,¹²⁸ T. K. Aarrestad,¹²⁹ D. Abbaneo,¹²⁹ J. Alimena,¹²⁹ E. Auffray,¹²⁹ G. Auzinger,¹²⁹ J. Baechler,¹²⁹ P. Baillon,^{129,a} A. H. Ball,¹²⁹ D. Barney,¹²⁹ J. Bendavid,¹²⁹ N. Beni,¹²⁹ M. Bianco,¹²⁹ A. Bocci,¹²⁹ E. Brondolin,¹²⁹ T. Camporesi,¹²⁹ M. Capeans Garrido,¹²⁹ G. Cerminara,¹²⁹ S. S. Chhibra,¹²⁹ L. Cristella,¹²⁹ D. d'Enterria,¹²⁹ A. Dabrowski,¹²⁹ N. Daci,¹²⁹ A. David,¹²⁹ A. De Roeck,¹²⁹ M. Deile,¹²⁹ R. Di Maria,¹²⁹ M. Dobson,¹²⁹ M. Dünser,¹²⁹ N. Dupont,¹²⁹ A. Elliott-Peisert,¹²⁹ N. Emriskova,¹²⁹ F. Fallavollita,^{129,iii} D. Fasanella,¹²⁹ S. Fiorendi,¹²⁹ A. Florent,¹²⁹ G. Franzoni,¹²⁹ J. Fulcher,¹²⁹ W. Funk,¹²⁹ S. Giani,¹²⁹ D. Gigi,¹²⁹ K. Gill,¹²⁹ F. Glege,¹²⁹ L. Gouskos,¹²⁹ M. Haranko,¹²⁹ J. Hegeman,¹²⁹ Y. Iiyama,¹²⁹ V. Innocente,¹²⁹ T. James,¹²⁹ P. Janot,¹²⁹ J. Kaspar,¹²⁹ J. Kieseler,¹²⁹ M. Komm,¹²⁹ N. Kratochwil,¹²⁹ C. Lange,¹²⁹ S. Laurila,¹²⁹ P. Lecoq,¹²⁹ K. Long,¹²⁹ C. Lourenço,¹²⁹ L. Malgeri,¹²⁹ S. Mallios,¹²⁹ M. Mannelli,¹²⁹ F. Meijers,¹²⁹ S. Mersi,¹²⁹ E. Meschi,¹²⁹ F. Moortgat,¹²⁹ M. Mulders,¹²⁹ S. Orfanelli,¹²⁹ L. Orsini,¹²⁹ F. Pantaleo,¹²⁹ L. Pape,¹²⁹ E. Perez,¹²⁹ M. Peruzzi,¹²⁹ A. Petrilli,¹²⁹ G. Petrucciani,¹²⁹ A. Pfeiffer,¹²⁹ M. Pierini,¹²⁹ M. Pitt,¹²⁹ H. Qu,¹²⁹ T. Quast,¹²⁹ D. Rabady,¹²⁹ A. Racz,¹²⁹ M. Rieger,¹²⁹ M. Rovere,¹²⁹ H. Sakulin,¹²⁹ J. Salfeld-Nebgen,¹²⁹ S. Scarfi,¹²⁹ C. Schäfer,¹²⁹ C. Schwick,¹²⁹ M. Selvaggi,¹²⁹ A. Sharma,¹²⁹ P. Silva,¹²⁹ W. Snoeys,¹²⁹ P. Sphicas,^{129,iii} S. Summers,¹²⁹ V. R. Tavolaro,¹²⁹ D. Treille,¹²⁹ A. Tsiros,¹²⁹ G. P. Van Onsem,¹²⁹ M. Verzetti,¹²⁹ K. A. Wozniak,¹²⁹ W. D. Zeuner,¹²⁹ L. Caminada,^{130,kkk} A. Ebrahimi,¹³⁰ W. Erdmann,¹³⁰ R. Horisberger,¹³⁰ Q. Ingram,¹³⁰ H. C. Kaestli,¹³⁰ D. Kotlinski,¹³⁰ U. Langenegger,¹³⁰ M. Missiroli,¹³⁰ T. Rohe,¹³⁰ K. Androsov,^{131,lll} M. Backhaus,¹³¹ P. Berger,¹³¹ A. Calandri,¹³¹ N. Chernyavskaya,¹³¹ A. De Cosa,¹³¹ G. Dissertori,¹³¹ M. Dittmar,¹³¹ M. Donegà,¹³¹ C. Dorfer,¹³¹ T. Gadek,¹³¹ T. A. Gómez Espinosa,¹³¹ C. Grab,¹³¹ D. Hits,¹³¹ W. Luster mann,¹³¹ A.-M. Lyon,¹³¹ R. A. Manzoni,¹³¹ C. Martin Perez,¹³¹ M. T. Meinhard,¹³¹ F. Micheli,¹³¹ F. Nessi-Tedaldi,¹³¹ J. Niedziela,¹³¹ F. Pauss,¹³¹ V. Perovic,¹³¹ G. Perrin,¹³¹ S. Pigazzini,¹³¹ M. G. Ratti,¹³¹ M. Reichmann,¹³¹ C. Reissel,¹³¹ T. Reitenspiess,¹³¹ B. Ristic,¹³¹ D. Ruini,¹³¹ D. A. Sanz Becerra,¹³¹ M. Schönenberger,¹³¹ V. Stampf,¹³¹ J. Steggemann,^{131,lll} R. Wallny,¹³¹ D. H. Zhu,¹³¹ C. Amsler,^{132,mmm} C. Botta,¹³² D. Brzhechko,¹³² M. F. Canelli,¹³² A. De Wit,¹³² R. Del Burgo,¹³² J. K. Heikkilä,¹³² M. Huwiler,¹³² A. Jofrehei,¹³² B. Kilminster,¹³² S. Leontsinis,¹³² A. Macchiolo,¹³² P. Meiring,¹³² V. M. Mikuni,¹³²

U. Molinatti,¹³² I. Neutelings,¹³² G. Rauco,¹³² A. Reimers,¹³² P. Robmann,¹³² S. Sanchez Cruz,¹³² K. Schweiger,¹³²
 Y. Takahashi,¹³² C. Adloff,^{133,nnn} C. M. Kuo,¹³³ W. Lin,¹³³ A. Roy,¹³³ T. Sarkar,^{133,ll} S. S. Yu,¹³³ L. Ceard,¹³⁴ P. Chang,¹³⁴
 Y. Chao,¹³⁴ K. F. Chen,¹³⁴ P. H. Chen,¹³⁴ W.-S. Hou,¹³⁴ Y. y. Li,¹³⁴ R.-S. Lu,¹³⁴ E. Paganis,¹³⁴ A. Psallidas,¹³⁴ A. Steen,¹³⁴
 E. Yazgan,¹³⁴ P. r. Yu,¹³⁴ B. Asavapibhop,¹³⁵ C. Asawatangtrakuldee,¹³⁵ N. Srimanobhas,¹³⁵ M. N. Bakirci,^{136,ooo}
 F. Boran,¹³⁶ S. Damarseckin,^{136,ppp} Z. S. Demiroglu,¹³⁶ F. Dolek,¹³⁶ I. Dumanoglu,^{136,qqq} G. Gokbulut,¹³⁶ Y. Guler,¹³⁶
 E. Gurpinar Guler,^{136,rrr} I. Hos,^{136,sss} C. Isik,¹³⁶ E. E. Kangal,^{136,ttt} O. Kara,¹³⁶ A. Kayis Topaksu,¹³⁶ U. Kiminsu,¹³⁶
 G. Onengut,¹³⁶ K. Ozdemir,^{136,uuu} A. E. Simsek,¹³⁶ B. Tali,^{136,vvv} U. G. Tok,¹³⁶ H. Topakli,^{136,www} S. Turkcapar,¹³⁶
 I. S. Zorbakir,¹³⁶ C. Zorbilmez,¹³⁶ B. Isildak,^{137,xxx} G. Karapinar,^{137,yyy} K. Ocalan,^{137,zzz} M. Yalvac,^{137,aaaa} B. Akgun,¹³⁸
 I. O. Atakisi,¹³⁸ E. Gülmez,¹³⁸ M. Kaya,^{138,bbbb} O. Kaya,^{138,cccc} Ö. Özçelik,¹³⁸ S. Tekten,^{138,dddd} E. A. Yetkin,^{138,eeee}
 A. Cakir,¹³⁹ K. Cankocak,^{139,qqq} Y. Komurcu,¹³⁹ S. Sen,^{139,fff} F. Aydogmus Sen,¹⁴⁰ S. Cerci,^{140,vvv} B. Kaynak,¹⁴⁰
 S. Ozkorucuklu,¹⁴⁰ D. Sunar Cerci,^{140,vvv} B. Grynyov,¹⁴¹ L. Levchuk,¹⁴² E. Bhal,¹⁴³ S. Bologna,¹⁴³ J. J. Brooke,¹⁴³
 A. Bundock,¹⁴³ E. Clement,¹⁴³ D. Cussans,¹⁴³ H. Flacher,¹⁴³ J. Goldstein,¹⁴³ G. P. Heath,¹⁴³ H. F. Heath,¹⁴³ L. Kreczko,¹⁴³
 B. Krikler,¹⁴³ S. Paramesvaran,¹⁴³ T. Sakuma,¹⁴³ S. Seif El Nasr-Storey,¹⁴³ V. J. Smith,¹⁴³ N. Stylianou,^{143,gggg} J. Taylor,¹⁴³
 A. Titterton,¹⁴³ K. W. Bell,¹⁴⁴ A. Belyaev,^{144,hhhh} C. Brew,¹⁴⁴ R. M. Brown,¹⁴⁴ D. J. A. Cockerill,¹⁴⁴ K. V. Ellis,¹⁴⁴
 K. Harder,¹⁴⁴ S. Harper,¹⁴⁴ J. Linacre,¹⁴⁴ K. Manolopoulos,¹⁴⁴ D. M. Newbold,¹⁴⁴ E. Olaiya,¹⁴⁴ D. Petyt,¹⁴⁴ T. Reis,¹⁴⁴
 T. Schuh,¹⁴⁴ C. H. Shepherd-Themistocleous,¹⁴⁴ A. Thea,¹⁴⁴ I. R. Tomalin,¹⁴⁴ T. Williams,¹⁴⁴ R. Bainbridge,¹⁴⁵ P. Bloch,¹⁴⁵
 S. Bonomally,¹⁴⁵ J. Borg,¹⁴⁵ S. Breeze,¹⁴⁵ O. Buchmuller,¹⁴⁵ V. Cepaitis,¹⁴⁵ G. S. Chahal,^{145,iiii} D. Colling,¹⁴⁵ P. Dauncey,¹⁴⁵
 G. Davies,¹⁴⁵ M. Della Negra,¹⁴⁵ S. Fayer,¹⁴⁵ G. Fedi,¹⁴⁵ G. Hall,¹⁴⁵ M. H. Hassanshahi,¹⁴⁵ G. Iles,¹⁴⁵ J. Langford,¹⁴⁵
 L. Lyons,¹⁴⁵ A.-M. Magnan,¹⁴⁵ S. Malik,¹⁴⁵ A. Martelli,¹⁴⁵ J. Nash,^{145,jjjj} V. Palladino,¹⁴⁵ M. Pesaresi,¹⁴⁵ D. M. Raymond,¹⁴⁵
 A. Richards,¹⁴⁵ A. Rose,¹⁴⁵ E. Scott,¹⁴⁵ C. Seez,¹⁴⁵ A. Shtipliyski,¹⁴⁵ A. Tapper,¹⁴⁵ K. Uchida,¹⁴⁵ T. Virdee,^{145,u} N. Wardle,¹⁴⁵
 S. N. Webb,¹⁴⁵ D. Winterbottom,¹⁴⁵ A. G. Zecchinelli,¹⁴⁵ J. E. Cole,¹⁴⁶ A. Khan,¹⁴⁶ P. Kyberd,¹⁴⁶ C. K. Mackay,¹⁴⁶
 I. D. Reid,¹⁴⁶ L. Teodorescu,¹⁴⁶ S. Zahid,¹⁴⁶ S. Abdullin,¹⁴⁷ A. Brinkerhoff,¹⁴⁷ B. Caraway,¹⁴⁷ J. Dittmann,¹⁴⁷
 K. Hatakeyama,¹⁴⁷ A. R. Kanuganti,¹⁴⁷ B. McMaster,¹⁴⁷ N. Pastika,¹⁴⁷ S. Sawant,¹⁴⁷ C. Smith,¹⁴⁷ C. Sutantawibul,¹⁴⁷
 J. Wilson,¹⁴⁷ R. Bartek,¹⁴⁸ A. Dominguez,¹⁴⁸ R. Uniyal,¹⁴⁸ A. M. Vargas Hernandez,¹⁴⁸ A. Buccilli,¹⁴⁹ O. Charaf,¹⁴⁹
 S. I. Cooper,¹⁴⁹ D. Di Croce,¹⁴⁹ S. V. Gleyzer,¹⁴⁹ C. Henderson,¹⁴⁹ C. U. Perez,¹⁴⁹ P. Rumerio,¹⁴⁹ C. West,¹⁴⁹ A. Akpinar,¹⁵⁰
 A. Albert,¹⁵⁰ D. Arcaro,¹⁵⁰ C. Cosby,¹⁵⁰ Z. Demiragli,¹⁵⁰ D. Gastler,¹⁵⁰ J. Rohlf,¹⁵⁰ K. Salyer,¹⁵⁰ D. Sperka,¹⁵⁰
 D. Spitzbart,¹⁵⁰ I. Suarez,¹⁵⁰ S. Yuan,¹⁵⁰ D. Zou,¹⁵⁰ G. Benelli,¹⁵¹ B. Burkle,¹⁵¹ X. Coubez,^{151,v} D. Cutts,¹⁵¹ Y. t. Duh,¹⁵¹
 M. Hadley,¹⁵¹ U. Heintz,¹⁵¹ J. M. Hogan,^{151,kkkk} K. H. M. Kwok,¹⁵¹ E. Laird,¹⁵¹ G. Landsberg,¹⁵¹ K. T. Lau,¹⁵¹ J. Lee,¹⁵¹
 J. Luo,¹⁵¹ M. Narain,¹⁵¹ S. Sagir,^{151,llll} E. Usai,¹⁵¹ W. Y. Wong,¹⁵¹ X. Yan,¹⁵¹ D. Yu,¹⁵¹ W. Zhang,¹⁵¹ C. Brainerd,¹⁵²
 R. Breedon,¹⁵² M. Calderon De La Barca Sanchez,¹⁵² M. Chertok,¹⁵² J. Conway,¹⁵² P. T. Cox,¹⁵² R. Erbacher,¹⁵²
 F. Jensen,¹⁵² O. Kukral,¹⁵² R. Lander,¹⁵² M. Mulhearn,¹⁵² D. Pellett,¹⁵² D. Taylor,¹⁵² M. Tripathi,¹⁵² Y. Yao,¹⁵² F. Zhang,¹⁵²
 M. Bachtis,¹⁵³ R. Cousins,¹⁵³ A. Dasgupta,¹⁵³ A. Datta,¹⁵³ D. Hamilton,¹⁵³ J. Hauser,¹⁵³ M. Ignatenko,¹⁵³ M. A. Iqbal,¹⁵³
 T. Lam,¹⁵³ N. Mccoll,¹⁵³ W. A. Nash,¹⁵³ S. Regnard,¹⁵³ D. Saltzberg,¹⁵³ C. Schnaible,¹⁵³ B. Stone,¹⁵³ V. Valuev,¹⁵³
 K. Burt,¹⁵⁴ Y. Chen,¹⁵⁴ R. Clare,¹⁵⁴ J. W. Gary,¹⁵⁴ G. Hanson,¹⁵⁴ G. Karapostoli,¹⁵⁴ O. R. Long,¹⁵⁴ N. Manganeli,¹⁵⁴
 M. Olmedo Negrete,¹⁵⁴ W. Si,¹⁵⁴ S. Wimpenny,¹⁵⁴ Y. Zhang,¹⁵⁴ J. G. Branson,¹⁵⁵ P. Chang,¹⁵⁵ S. Cittolin,¹⁵⁵
 S. Cooperstein,¹⁵⁵ N. Deelen,¹⁵⁵ J. Duarte,¹⁵⁵ R. Gerosa,¹⁵⁵ L. Giannini,¹⁵⁵ D. Gilbert,¹⁵⁵ J. Guiang,¹⁵⁵ R. Kansal,¹⁵⁵
 V. Krutelyov,¹⁵⁵ R. Lee,¹⁵⁵ J. Letts,¹⁵⁵ M. Masciovecchio,¹⁵⁵ S. May,¹⁵⁵ S. Padhi,¹⁵⁵ M. Pieri,¹⁵⁵ B. V. Sathia Narayanan,¹⁵⁵
 V. Sharma,¹⁵⁵ M. Tadel,¹⁵⁵ A. Vartak,¹⁵⁵ F. Würthwein,¹⁵⁵ Y. Xiang,¹⁵⁵ A. Yagil,¹⁵⁵ N. Amin,¹⁵⁶ C. Campagnari,¹⁵⁶
 M. Citron,¹⁵⁶ A. Dorsett,¹⁵⁶ V. Dutta,¹⁵⁶ J. Incandela,¹⁵⁶ M. Kilpatrick,¹⁵⁶ B. Marsh,¹⁵⁶ H. Mei,¹⁵⁶ A. Ovcharova,¹⁵⁶
 M. Quinnan,¹⁵⁶ J. Richman,¹⁵⁶ U. Sarica,¹⁵⁶ D. Stuart,¹⁵⁶ S. Wang,¹⁵⁶ A. Bornheim,¹⁵⁷ O. Cerri,¹⁵⁷ I. Dutta,¹⁵⁷
 J. M. Lawhorn,¹⁵⁷ N. Lu,¹⁵⁷ J. Mao,¹⁵⁷ H. B. Newman,¹⁵⁷ J. Ngadiuba,¹⁵⁷ T. Q. Nguyen,¹⁵⁷ M. Spiropulu,¹⁵⁷
 J. R. Vlimant,¹⁵⁷ C. Wang,¹⁵⁷ S. Xie,¹⁵⁷ Z. Zhang,¹⁵⁷ R. Y. Zhu,¹⁵⁷ J. Alison,¹⁵⁸ M. B. Andrews,¹⁵⁸ T. Ferguson,¹⁵⁸
 T. Mudholkar,¹⁵⁸ M. Paulini,¹⁵⁸ I. Vorobiev,¹⁵⁸ J. P. Cumalat,¹⁵⁹ W. T. Ford,¹⁵⁹ E. MacDonald,¹⁵⁹ R. Patel,¹⁵⁹ A. Perloff,¹⁵⁹
 K. Stenson,¹⁵⁹ K. A. Ulmer,¹⁵⁹ S. R. Wagner,¹⁵⁹ J. Alexander,¹⁶⁰ Y. Cheng,¹⁶⁰ J. Chu,¹⁶⁰ D. J. Cranshaw,¹⁶⁰ K. McDermott,¹⁶⁰
 J. Monroy,¹⁶⁰ J. R. Patterson,¹⁶⁰ D. Quach,¹⁶⁰ A. Ryd,¹⁶⁰ W. Sun,¹⁶⁰ S. M. Tan,¹⁶⁰ Z. Tao,¹⁶⁰ J. Thom,¹⁶⁰ P. Wittich,¹⁶⁰
 M. Zientek,¹⁶⁰ M. Albrow,¹⁶¹ M. Alyari,¹⁶¹ G. Apollinari,¹⁶¹ A. Apresyan,¹⁶¹ A. Apyan,¹⁶¹ S. Banerjee,¹⁶¹
 L. A. T. Bauerdick,¹⁶¹ A. Beretvas,¹⁶¹ D. Berry,¹⁶¹ J. Berryhill,¹⁶¹ P. C. Bhat,¹⁶¹ K. Burkett,¹⁶¹ J. N. Butler,¹⁶¹ A. Canepa,¹⁶¹
 G. B. Cerati,¹⁶¹ H. W. K. Cheung,¹⁶¹ F. Chlebana,¹⁶¹ M. Cremonesi,¹⁶¹ K. F. Di Petrillo,¹⁶¹ V. D. Elvira,¹⁶¹ J. Freeman,¹⁶¹
 Z. Gece,¹⁶¹ L. Gray,¹⁶¹ D. Green,¹⁶¹ S. Grünendahl,¹⁶¹ O. Gutsche,¹⁶¹ R. M. Harris,¹⁶¹ R. Heller,¹⁶¹ T. C. Herwig,¹⁶¹

J. Hirschauer,¹⁶¹ B. Jayatilaka,¹⁶¹ S. Jindariani,¹⁶¹ M. Johnson,¹⁶¹ U. Joshi,¹⁶¹ P. Klabbers,¹⁶¹ T. Klijnsmas,¹⁶¹ B. Klima,¹⁶¹ M. J. Kortelainen,¹⁶¹ S. Lammel,¹⁶¹ D. Lincoln,¹⁶¹ R. Lipton,¹⁶¹ T. Liu,¹⁶¹ J. Lykken,¹⁶¹ C. Madrid,¹⁶¹ K. Maeshima,¹⁶¹ C. Mantilla,¹⁶¹ D. Mason,¹⁶¹ P. McBride,¹⁶¹ P. Merkel,¹⁶¹ S. Mrenna,¹⁶¹ S. Nahn,¹⁶¹ V. O'Dell,¹⁶¹ V. Papadimitriou,¹⁶¹ K. Pedro,¹⁶¹ C. Pena,^{161,eee} O. Prokofyev,¹⁶¹ F. Ravera,¹⁶¹ A. Reinsvold Hall,¹⁶¹ L. Ristori,¹⁶¹ B. Schneider,¹⁶¹ E. Sexton-Kennedy,¹⁶¹ N. Smith,¹⁶¹ A. Soha,¹⁶¹ L. Spiegel,¹⁶¹ S. Stoynev,¹⁶¹ J. Strait,¹⁶¹ L. Taylor,¹⁶¹ S. Tkaczyk,¹⁶¹ N. V. Tran,¹⁶¹ L. Uplegger,¹⁶¹ E. W. Vaandering,¹⁶¹ H. A. Weber,¹⁶¹ A. Woodard,¹⁶¹ D. Acosta,¹⁶² P. Avery,¹⁶² D. Bourilkov,¹⁶² L. Cadamuro,¹⁶² V. Cherepanov,¹⁶² F. Errico,¹⁶² R. D. Field,¹⁶² D. Guerrero,¹⁶² B. M. Joshi,¹⁶² M. Kim,¹⁶² J. Konigsberg,¹⁶² A. Korytov,¹⁶² K. H. Lo,¹⁶² K. Matchev,¹⁶² N. Menendez,¹⁶² G. Mitselmakher,¹⁶² D. Rosenzweig,¹⁶² K. Shi,¹⁶² J. Sturdy,¹⁶² J. Wang,¹⁶² E. Yigitbasi,¹⁶² X. Zuo,¹⁶² T. Adams,¹⁶³ A. Askew,¹⁶³ D. Diaz,¹⁶³ R. Habibullah,¹⁶³ S. Hagopian,¹⁶³ V. Hagopian,¹⁶³ K. F. Johnson,¹⁶³ R. Khurana,¹⁶³ T. Kolberg,¹⁶³ G. Martinez,¹⁶³ H. Prosper,¹⁶³ C. Schiber,¹⁶³ R. Yohay,¹⁶³ J. Zhang,¹⁶³ M. M. Baarmand,¹⁶⁴ S. Butalla,¹⁶⁴ T. Elkafrawy,^{164,o} M. Hohlmann,¹⁶⁴ R. Kumar Verma,¹⁶⁴ D. Noonan,¹⁶⁴ M. Rahmani,¹⁶⁴ M. Saunders,¹⁶⁴ F. Yumiceva,¹⁶⁴ M. R. Adams,¹⁶⁵ L. Apanasevich,¹⁶⁵ H. Becerril Gonzalez,¹⁶⁵ R. Cavanaugh,¹⁶⁵ X. Chen,¹⁶⁵ S. Dittmer,¹⁶⁵ O. Evdokimov,¹⁶⁵ C. E. Gerber,¹⁶⁵ D. A. Hangal,¹⁶⁵ D. J. Hofman,¹⁶⁵ C. Mills,¹⁶⁵ G. Oh,¹⁶⁵ T. Roy,¹⁶⁵ M. B. Tonjes,¹⁶⁵ N. Varelas,¹⁶⁵ J. Viinikainen,¹⁶⁵ X. Wang,¹⁶⁵ Z. Wu,¹⁶⁵ Z. Ye,¹⁶⁵ M. Alhusseini,¹⁶⁶ K. Dilsiz,^{166,mmmm} S. Durgut,¹⁶⁶ R. P. Gandrajula,¹⁶⁶ M. Haytmyradov,¹⁶⁶ V. Khristenko,¹⁶⁶ O. K. Köseyan,¹⁶⁶ J.-P. Merlo,¹⁶⁶ A. Mestvirishvili,^{166,nnnn} A. Moeller,¹⁶⁶ J. Nachtman,¹⁶⁶ H. Ogul,^{166,oooo} Y. Onel,¹⁶⁶ F. Ozok,^{166,pppp} A. Penzo,¹⁶⁶ C. Snyder,¹⁶⁶ E. Tiras,^{166,qqqq} J. Wetzel,¹⁶⁶ O. Amram,¹⁶⁷ B. Blumenfeld,¹⁶⁷ L. Corcodilos,¹⁶⁷ M. Eminizer,¹⁶⁷ A. V. Gritsan,¹⁶⁷ S. Kyriacou,¹⁶⁷ P. Maksimovic,¹⁶⁷ J. Roskes,¹⁶⁷ M. Swartz,¹⁶⁷ T. Á. Vámi,¹⁶⁷ C. Baldenegro Barrera,¹⁶⁸ P. Baringer,¹⁶⁸ A. Bean,¹⁶⁸ A. Bylinkin,¹⁶⁸ T. Isidori,¹⁶⁸ S. Khalil,¹⁶⁸ J. King,¹⁶⁸ G. Krintiras,¹⁶⁸ A. Kropivnitskaya,¹⁶⁸ C. Lindsey,¹⁶⁸ N. Minafra,¹⁶⁸ M. Murray,¹⁶⁸ C. Rogan,¹⁶⁸ C. Royon,¹⁶⁸ S. Sanders,¹⁶⁸ E. Schmitz,¹⁶⁸ J. D. Tapia Takaki,¹⁶⁸ Q. Wang,¹⁶⁸ J. Williams,¹⁶⁸ G. Wilson,¹⁶⁸ S. Duric,¹⁶⁹ A. Ivanov,¹⁶⁹ K. Kaadze,¹⁶⁹ D. Kim,¹⁶⁹ Y. Maravin,¹⁶⁹ T. Mitchell,¹⁶⁹ A. Modak,¹⁶⁹ K. Nam,¹⁶⁹ F. Rebassoo,¹⁷⁰ D. Wright,¹⁷⁰ E. Adams,¹⁷¹ A. Baden,¹⁷¹ O. Baron,¹⁷¹ A. Belloni,¹⁷¹ S. C. Eno,¹⁷¹ Y. Feng,¹⁷¹ N. J. Hadley,¹⁷¹ S. Jabeen,¹⁷¹ R. G. Kellogg,¹⁷¹ T. Koeth,¹⁷¹ A. C. Mignerey,¹⁷¹ S. Nabili,¹⁷¹ M. Seidel,¹⁷¹ A. Skuja,¹⁷¹ S. C. Tonwar,¹⁷¹ L. Wang,¹⁷¹ K. Wong,¹⁷¹ D. Abercrombie,¹⁷² G. Andreassi,¹⁷² R. Bi,¹⁷² S. Brandt,¹⁷² W. Busza,¹⁷² I. A. Cali,¹⁷² Y. Chen,¹⁷² M. D'Alfonso,¹⁷² G. Gomez Ceballos,¹⁷² M. Goncharov,¹⁷² P. Harris,¹⁷² M. Hu,¹⁷² M. Klute,¹⁷² D. Kovalskyi,¹⁷² J. Krupa,¹⁷² Y.-J. Lee,¹⁷² B. Maier,¹⁷² A. C. Marini,¹⁷² C. Mironov,¹⁷² C. Paus,¹⁷² D. Rankin,¹⁷² C. Roland,¹⁷² G. Roland,¹⁷² Z. Shi,¹⁷² G. S. F. Stephens,¹⁷² K. Tatar,¹⁷² J. Wang,¹⁷² Z. Wang,¹⁷² B. Wyslouch,¹⁷² R. M. Chatterjee,¹⁷³ A. Evans,¹⁷³ P. Hansen,¹⁷³ J. Hiltbrand,¹⁷³ Sh. Jain,¹⁷³ M. Krohn,¹⁷³ Y. Kubota,¹⁷³ Z. Lesko,¹⁷³ J. Mans,¹⁷³ M. Revering,¹⁷³ R. Rusack,¹⁷³ R. Saradhy,¹⁷³ N. Schroeder,¹⁷³ N. Strobbe,¹⁷³ M. A. Wadud,¹⁷³ J. G. Acosta,¹⁷⁴ S. Oliveros,¹⁷⁴ K. Bloom,¹⁷⁵ M. Bryson,¹⁷⁵ S. Chauhan,¹⁷⁵ D. R. Claes,¹⁷⁵ C. Fangmeier,¹⁷⁵ L. Finco,¹⁷⁵ F. Golf,¹⁷⁵ J. R. González Fernández,¹⁷⁵ C. Joo,¹⁷⁵ I. Kravchenko,¹⁷⁵ J. E. Siado,¹⁷⁵ G. R. Snow,^{175,a} W. Tabb,¹⁷⁵ F. Yan,¹⁷⁵ G. Agarwal,¹⁷⁶ H. Bandyopadhyay,¹⁷⁶ L. Hay,¹⁷⁶ I. Iashvili,¹⁷⁶ A. Kharchilava,¹⁷⁶ C. McLean,¹⁷⁶ D. Nguyen,¹⁷⁶ J. Pekkanen,¹⁷⁶ S. Rappoccio,¹⁷⁶ A. Williams,¹⁷⁶ G. Alverson,¹⁷⁷ E. Barberis,¹⁷⁷ C. Freer,¹⁷⁷ Y. Haddad,¹⁷⁷ A. Hortiangtham,¹⁷⁷ J. Li,¹⁷⁷ G. Madigan,¹⁷⁷ B. Marzocchi,¹⁷⁷ D. M. Morse,¹⁷⁷ V. Nguyen,¹⁷⁷ T. Orimoto,¹⁷⁷ A. Parker,¹⁷⁷ L. Skinnari,¹⁷⁷ A. Tishelman-Charny,¹⁷⁷ T. Wamorkar,¹⁷⁷ B. Wang,¹⁷⁷ A. Wisecarver,¹⁷⁷ D. Wood,¹⁷⁷ S. Bhattacharya,¹⁷⁸ J. Bueghly,¹⁷⁸ Z. Chen,¹⁷⁸ A. Gilbert,¹⁷⁸ T. Gunter,¹⁷⁸ K. A. Hahn,¹⁷⁸ N. Odell,¹⁷⁸ M. H. Schmitt,¹⁷⁸ K. Sung,¹⁷⁸ M. Velasco,¹⁷⁸ R. Band,¹⁷⁹ R. Bucci,¹⁷⁹ N. Dev,¹⁷⁹ R. Goldouzian,¹⁷⁹ M. Hildreth,¹⁷⁹ K. Hurtado Anampa,¹⁷⁹ C. Jessop,¹⁷⁹ K. Lannon,¹⁷⁹ N. Loukas,¹⁷⁹ N. Marinelli,¹⁷⁹ I. Mcalister,¹⁷⁹ F. Meng,¹⁷⁹ K. Mohrman,¹⁷⁹ Y. Musienko,^{179,xx} R. Ruchti,¹⁷⁹ P. Siddireddy,¹⁷⁹ M. Wayne,¹⁷⁹ A. Wightman,¹⁷⁹ M. Wolf,¹⁷⁹ M. Zarucki,¹⁷⁹ L. Zygala,¹⁷⁹ B. Bylsma,¹⁸⁰ B. Cardwell,¹⁸⁰ L. S. Durkin,¹⁸⁰ B. Francis,¹⁸⁰ C. Hill,¹⁸⁰ A. Lefeld,¹⁸⁰ B. L. Winer,¹⁸⁰ B. R. Yates,¹⁸⁰ F. M. Addesa,¹⁸¹ B. Bonham,¹⁸¹ P. Das,¹⁸¹ G. Dezoort,¹⁸¹ P. Elmer,¹⁸¹ A. Frankenthal,¹⁸¹ B. Greenberg,¹⁸¹ N. Haubrich,¹⁸¹ S. Higginbotham,¹⁸¹ A. Kalogeropoulos,¹⁸¹ G. Kopp,¹⁸¹ S. Kwan,¹⁸¹ D. Lange,¹⁸¹ M. T. Lucchini,¹⁸¹ D. Marlow,¹⁸¹ K. Mei,¹⁸¹ I. Ojalvo,¹⁸¹ J. Olsen,¹⁸¹ C. Palmer,¹⁸¹ D. Stickland,¹⁸¹ C. Tully,¹⁸¹ S. Malik,¹⁸² S. Norberg,¹⁸² A. S. Bakshi,¹⁸³ V. E. Barnes,¹⁸³ R. Chawla,¹⁸³ S. Das,¹⁸³ L. Gutay,¹⁸³ M. Jones,¹⁸³ A. W. Jung,¹⁸³ S. Karmarkar,¹⁸³ M. Liu,¹⁸³ G. Negro,¹⁸³ N. Neumeister,¹⁸³ G. Paspalaki,¹⁸³ C. C. Peng,¹⁸³ S. Piperov,¹⁸³ A. Purohit,¹⁸³ J. F. Schulte,¹⁸³ M. Stojanovic,^{183,r} J. Thieman,¹⁸³ F. Wang,¹⁸³ R. Xiao,¹⁸³ W. Xie,¹⁸³ J. Dolen,¹⁸⁴ N. Parashar,¹⁸⁴ A. Baty,¹⁸⁵ S. Dildick,¹⁸⁵ K. M. Ecklund,¹⁸⁵ S. Freed,¹⁸⁵ F. J. M. Geurts,¹⁸⁵ A. Kumar,¹⁸⁵ W. Li,¹⁸⁵ B. P. Padley,¹⁸⁵ R. Redjimi,¹⁸⁵ J. Roberts,^{185,a} W. Shi,¹⁸⁵ A. G. Stahl Leiton,¹⁸⁵ A. Bodek,¹⁸⁶ P. de Barbaro,¹⁸⁶ R. Demina,¹⁸⁶ J. L. Dulemba,¹⁸⁶ C. Fallon,¹⁸⁶ T. Ferbel,¹⁸⁶ M. Galanti,¹⁸⁶ A. Garcia-Bellido,¹⁸⁶ O. Hindrichs,¹⁸⁶ A. Khukhunaishvili,¹⁸⁶ E. Ranken,¹⁸⁶ R. Taus,¹⁸⁶

B. Chiarito,¹⁸⁷ J. P. Chou,¹⁸⁷ A. Gandrakota,¹⁸⁷ Y. Gershtein,¹⁸⁷ E. Halkiadakis,¹⁸⁷ A. Hart,¹⁸⁷ M. Heindl,¹⁸⁷ E. Hughes,¹⁸⁷ S. Kaplan,¹⁸⁷ O. Karacheban,^{187,y} I. Laflotte,¹⁸⁷ A. Lath,¹⁸⁷ R. Montalvo,¹⁸⁷ K. Nash,¹⁸⁷ M. Osherson,¹⁸⁷ S. Salur,¹⁸⁷ S. Schnetzer,¹⁸⁷ S. Somalwar,¹⁸⁷ R. Stone,¹⁸⁷ S. A. Thayil,¹⁸⁷ S. Thomas,¹⁸⁷ H. Wang,¹⁸⁷ H. Acharya,¹⁸⁸ A. G. Delannoy,¹⁸⁸ S. Spanier,¹⁸⁸ O. Bouhali,^{189,rrr} M. Dalchenko,¹⁸⁹ A. Delgado,¹⁸⁹ R. Eusebi,¹⁸⁹ J. Gilmore,¹⁸⁹ T. Huang,¹⁸⁹ T. Kamon,^{189,sss} H. Kim,¹⁸⁹ S. Luo,¹⁸⁹ S. Malhotra,¹⁸⁹ R. Mueller,¹⁸⁹ D. Overton,¹⁸⁹ D. Rathjens,¹⁸⁹ A. Safonov,¹⁸⁹ N. Akchurin,¹⁹⁰ J. Damgov,¹⁹⁰ V. Hegde,¹⁹⁰ S. Kunori,¹⁹⁰ K. Lamichhane,¹⁹⁰ S. W. Lee,¹⁹⁰ T. Mengke,¹⁹⁰ S. Muthumuni,¹⁹⁰ T. Peltola,¹⁹⁰ S. Undleeb,¹⁹⁰ I. Volobouev,¹⁹⁰ Z. Wang,¹⁹⁰ A. Whitbeck,¹⁹⁰ E. Appelt,¹⁹¹ S. Greene,¹⁹¹ A. Gurrola,¹⁹¹ W. Johns,¹⁹¹ C. Maguire,¹⁹¹ A. Melo,¹⁹¹ H. Ni,¹⁹¹ K. Padeken,¹⁹¹ F. Romeo,¹⁹¹ P. Sheldon,¹⁹¹ S. Tuo,¹⁹¹ J. Velkovska,¹⁹¹ M. W. Arenton,¹⁹² B. Cox,¹⁹² G. Cummings,¹⁹² J. Hakala,¹⁹² R. Hirosky,¹⁹² M. Joyce,¹⁹² A. Ledovsky,¹⁹² A. Li,¹⁹² C. Neu,¹⁹² B. Tannenwald,¹⁹² E. Wolfe,¹⁹² P. E. Karchin,¹⁹³ N. Poudyal,¹⁹³ P. Thapa,¹⁹³ K. Black,¹⁹⁴ T. Bose,¹⁹⁴ J. Buchanan,¹⁹⁴ C. Caillol,¹⁹⁴ S. Dasu,¹⁹⁴ I. De Bruyn,¹⁹⁴ P. Everaerts,¹⁹⁴ F. Fienga,¹⁹⁴ C. Galloni,¹⁹⁴ H. He,¹⁹⁴ M. Herndon,¹⁹⁴ A. Hervé,¹⁹⁴ U. Hussain,¹⁹⁴ A. Lanaro,¹⁹⁴ A. Loeliger,¹⁹⁴ R. Loveless,¹⁹⁴ J. Madhusudanan Sreekala,¹⁹⁴ A. Mallampalli,¹⁹⁴ A. Mohammadi,¹⁹⁴ D. Pinna,¹⁹⁴ A. Savin,¹⁹⁴ V. Shang,¹⁹⁴ V. Sharma,¹⁹⁴ W. H. Smith,¹⁹⁴ D. Teague,¹⁹⁴ S. Trembath-Reichert,¹⁹⁴ and W. Vetens¹⁹⁴

(CMS Collaboration)

¹*Yerevan Physics Institute, Yerevan, Armenia*

²*Institut für Hochenergiephysik, Wien, Austria*

³*Institute for Nuclear Problems, Minsk, Belarus*

⁴*Universiteit Antwerpen, Antwerpen, Belgium*

⁵*Vrije Universiteit Brussel, Brussel, Belgium*

⁶*Université Libre de Bruxelles, Bruxelles, Belgium*

⁷*Ghent University, Ghent, Belgium*

⁸*Université Catholique de Louvain, Louvain-la-Neuve, Belgium*

⁹*Centro Brasileiro de Pesquisas Físicas, Rio de Janeiro, Brazil*

¹⁰*Universidade do Estado do Rio de Janeiro, Rio de Janeiro, Brazil*

^{11a}*Universidade Estadual Paulista, São Paulo, Brazil*

^{11b}*Universidade Federal do ABC, São Paulo, Brazil*

¹²*Institute for Nuclear Research and Nuclear Energy, Bulgarian Academy of Sciences, Sofia, Bulgaria*

¹³*University of Sofia, Sofia, Bulgaria*

¹⁴*Beihang University, Beijing, China*

¹⁵*Department of Physics, Tsinghua University, Beijing, China*

¹⁶*Institute of High Energy Physics, Beijing, China*

¹⁷*State Key Laboratory of Nuclear Physics and Technology, Peking University, Beijing, China*

¹⁸*Sun Yat-Sen University, Guangzhou, China*

¹⁹*Institute of Modern Physics and Key Laboratory of Nuclear Physics and Ion-beam Application (MOE)—Fudan University, Shanghai, China*

²⁰*Zhejiang University, Hangzhou, China*

²¹*Universidad de Los Andes, Bogota, Colombia*

²²*Universidad de Antioquia, Medellin, Colombia*

²³*University of Split, Faculty of Electrical Engineering, Mechanical Engineering and Naval Architecture, Split, Croatia*

²⁴*University of Split, Faculty of Science, Split, Croatia*

²⁵*Institute Rudjer Boskovic, Zagreb, Croatia*

²⁶*University of Cyprus, Nicosia, Cyprus*

²⁷*Charles University, Prague, Czech Republic*

²⁸*Escuela Politécnica Nacional, Quito, Ecuador*

²⁹*Universidad San Francisco de Quito, Quito, Ecuador*

³⁰*Academy of Scientific Research and Technology of the Arab Republic of Egypt, Egyptian Network of High Energy Physics, Cairo, Egypt*

³¹*Center for High Energy Physics (CHEP-FU), Fayoum University, El-Fayoum, Egypt*

³²*National Institute of Chemical Physics and Biophysics, Tallinn, Estonia*

³³*Department of Physics, University of Helsinki, Helsinki, Finland*

³⁴*Helsinki Institute of Physics, Helsinki, Finland*

³⁵*Lappeenranta University of Technology, Lappeenranta, Finland*

- ³⁶*IRFU, CEA, Université Paris-Saclay, Gif-sur-Yvette, France*
- ³⁷*Laboratoire Leprince-Ringuet, CNRS/IN2P3, Ecole Polytechnique, Institut Polytechnique de Paris, Palaiseau, France*
- ³⁸*Université de Strasbourg, CNRS, IPHC UMR 7178, Strasbourg, France*
- ³⁹*Institut de Physique des 2 Infinis de Lyon (IP2I), Villeurbanne, France*
- ⁴⁰*Georgian Technical University, Tbilisi, Georgia*
- ⁴¹*RWTH Aachen University, I. Physikalisches Institut, Aachen, Germany*
- ⁴²*RWTH Aachen University, III. Physikalisches Institut A, Aachen, Germany*
- ⁴³*RWTH Aachen University, III. Physikalisches Institut B, Aachen, Germany*
- ⁴⁴*Deutsches Elektronen-Synchrotron, Hamburg, Germany*
- ⁴⁵*University of Hamburg, Hamburg, Germany*
- ⁴⁶*Karlsruher Institut fuer Technologie, Karlsruhe, Germany*
- ⁴⁷*Institute of Nuclear and Particle Physics (INPP), NCSR Demokritos, Aghia Paraskevi, Greece*
- ⁴⁸*National and Kapodistrian University of Athens, Athens, Greece*
- ⁴⁹*National Technical University of Athens, Athens, Greece*
- ⁵⁰*University of Ioánnina, Ioánnina, Greece*
- ⁵¹*MTA-ELTE Lendület CMS Particle and Nuclear Physics Group, Eötvös Loránd University, Budapest, Hungary*
- ⁵²*Wigner Research Centre for Physics, Budapest, Hungary*
- ⁵³*Institute of Nuclear Research ATOMKI, Debrecen, Hungary*
- ⁵⁴*Institute of Physics, University of Debrecen, Debrecen, Hungary*
- ⁵⁵*Eszterhazy Karoly University, Karoly Robert Campus, Gyongyos, Hungary*
- ⁵⁶*Indian Institute of Science (IISc), Bangalore, India*
- ⁵⁷*National Institute of Science Education and Research, HBNI, Bhubaneswar, India*
- ⁵⁸*Panjab University, Chandigarh, India*
- ⁵⁹*University of Delhi, Delhi, India*
- ⁶⁰*Saha Institute of Nuclear Physics, HBNI, Kolkata, India*
- ⁶¹*Indian Institute of Technology Madras, Madras, India*
- ⁶²*Bhabha Atomic Research Centre, Mumbai, India*
- ⁶³*Tata Institute of Fundamental Research-A, Mumbai, India*
- ⁶⁴*Tata Institute of Fundamental Research-B, Mumbai, India*
- ⁶⁵*Indian Institute of Science Education and Research (IISER), Pune, India*
- ⁶⁶*Department of Physics, Isfahan University of Technology, Isfahan, Iran*
- ⁶⁷*Institute for Research in Fundamental Sciences (IPM), Tehran, Iran*
- ⁶⁸*University College Dublin, Dublin, Ireland*
- ^{69a}*INFN Sezione di Bari, Bari, Italy*
- ^{69b}*Università di Bari, Bari, Italy*
- ^{69c}*Politecnico di Bari, Bari, Italy*
- ^{70a}*INFN Sezione di Bologna, Bologna, Italy*
- ^{70b}*Università di Bologna, Bologna, Italy*
- ^{71a}*INFN Sezione di Catania*
- ^{71b}*Università di Catania*
- ^{72a}*INFN Sezione di Firenze, Firenze, Italy*
- ^{72b}*Università di Firenze, Firenze, Italy*
- ⁷³*INFN Laboratori Nazionali di Frascati, Frascati, Italy*
- ^{74a}*INFN Sezione di Genova*
- ^{74b}*Università di Genova*
- ^{75a}*INFN Sezione di Milano-Bicocca, Milano, Italy*
- ^{75b}*Università di Milano-Bicocca, Milano, Italy*
- ^{76a}*INFN Sezione di Napoli, Napoli, Italy*
- ^{76b}*Università di Napoli 'Federico II', Napoli, Italy*
- ^{76c}*Università della Basilicata, Napoli, Italy*
- ^{76d}*Università G. Marconi*
- ^{77a}*INFN Sezione di Padova*
- ^{77b}*Università di Padova*
- ^{77c}*Università di Trento*
- ^{78a}*INFN Sezione di Pavia, Pavia, Italy*
- ^{78b}*Università di Pavia, Pavia, Italy*
- ^{79a}*INFN Sezione di Perugia, Perugia, Italy*
- ^{79b}*Università di Perugia, Perugia, Italy*

- ^{80a}*INFN Sezione di Pisa, Pisa, Italy*
^{80b}*Università di Pisa, Pisa, Italy*
^{80c}*Scuola Normale Superiore di Pisa, Pisa, Italy*
^{80d}*Università di Siena, Siena, Italy*
^{81a}*INFN Sezione di Roma, Roma, Italy*
^{81b}*Sapienza Università di Roma, Roma, Italy*
^{82a}*INFN Sezione di Torino, Torino, Italy*
^{82b}*Università di Torino, Torino, Italy*
^{82c}*Università del Piemonte Orientale, Novara, Italy*
^{83a}*INFN Sezione di Trieste, Trieste, Italy*
^{83b}*Università di Trieste, Trieste, Italy*
⁸⁴*Kyungpook National University, Daegu, Korea*
⁸⁵*Chonnam National University, Institute for Universe and Elementary Particles, Kwangju, Korea*
⁸⁶*Hanyang University, Seoul, Korea*
⁸⁷*Korea University, Seoul, Korea*
⁸⁸*Kyung Hee University, Department of Physics, Seoul, Republic of Korea*
⁸⁹*Sejong University, Seoul, Korea*
⁹⁰*Seoul National University, Seoul, Korea*
⁹¹*University of Seoul, Seoul, Korea*
⁹²*Yonsei University, Department of Physics, Seoul, Korea*
⁹³*Sungkyunkwan University, Suwon, Korea*
⁹⁴*College of Engineering and Technology, American University of the Middle East (AUM), Egaila, Kuwait*
⁹⁵*Riga Technical University, Riga, Latvia*
⁹⁶*Vilnius University, Vilnius, Lithuania*
⁹⁷*National Centre for Particle Physics, Universiti Malaya, Kuala Lumpur, Malaysia*
⁹⁸*Universidad de Sonora (UNISON), Hermosillo, Mexico*
⁹⁹*Centro de Investigacion y de Estudios Avanzados del IPN, Mexico City, Mexico*
¹⁰⁰*Universidad Iberoamericana, Mexico City, Mexico*
¹⁰¹*Benemerita Universidad Autonoma de Puebla, Puebla, Mexico*
¹⁰²*University of Montenegro, Podgorica, Montenegro*
¹⁰³*University of Auckland, Auckland, New Zealand*
¹⁰⁴*University of Canterbury, Christchurch, New Zealand*
¹⁰⁵*National Centre for Physics, Quaid-I-Azam University, Islamabad, Pakistan*
¹⁰⁶*AGH University of Science and Technology Faculty of Computer Science, Electronics and Telecommunications, Krakow, Poland*
¹⁰⁷*National Centre for Nuclear Research, Swierk, Poland*
¹⁰⁸*Institute of Experimental Physics, Faculty of Physics, University of Warsaw, Warsaw, Poland*
¹⁰⁹*Laboratório de Instrumentação e Física Experimental de Partículas, Lisboa, Portugal*
¹¹⁰*Joint Institute for Nuclear Research, Dubna, Russia*
¹¹¹*Petersburg Nuclear Physics Institute, Gatchina (St. Petersburg), Russia*
¹¹²*Institute for Nuclear Research, Moscow, Russia*
¹¹³*Institute for Theoretical and Experimental Physics named by A.I. Alikhanov of NRC ‘Kurchatov Institute’, Moscow, Russia*
¹¹⁴*Moscow Institute of Physics and Technology, Moscow, Russia*
¹¹⁵*National Research Nuclear University ‘Moscow Engineering Physics Institute’ (MEPhI), Moscow, Russia*
¹¹⁶*P.N. Lebedev Physical Institute, Moscow, Russia*
¹¹⁷*Skobeltsyn Institute of Nuclear Physics, Lomonosov Moscow State University, Moscow, Russia*
¹¹⁸*Novosibirsk State University (NSU), Novosibirsk, Russia*
¹¹⁹*Institute for High Energy Physics of National Research Centre ‘Kurchatov Institute’, Protvino, Russia*
¹²⁰*National Research Tomsk Polytechnic University, Tomsk, Russia*
¹²¹*Tomsk State University, Tomsk, Russia*
¹²²*University of Belgrade: Faculty of Physics and VINCA Institute of Nuclear Sciences, Belgrade, Serbia*
¹²³*Centro de Investigaciones Energéticas Medioambientales y Tecnológicas (CIEMAT), Madrid, Spain*
¹²⁴*Universidad Autónoma de Madrid, Madrid, Spain*
¹²⁵*Universidad de Oviedo, Instituto Universitario de Ciencias y Tecnologías Espaciales de Asturias (ICTEA), Oviedo, Spain*
¹²⁶*Instituto de Física de Cantabria (IFCA), CSIC-Universidad de Cantabria, Santander, Spain*
¹²⁷*University of Colombo, Colombo, Sri Lanka*
¹²⁸*University of Ruhuna, Department of Physics, Matara, Sri Lanka*

- ¹²⁹*CERN, European Organization for Nuclear Research, Geneva, Switzerland*
¹³⁰*Paul Scherrer Institut, Villigen, Switzerland*
¹³¹*ETH Zurich—Institute for Particle Physics and Astrophysics (IPA), Zurich, Switzerland*
¹³²*Universität Zürich, Zurich, Switzerland*
¹³³*National Central University, Chung-Li, Taiwan*
¹³⁴*National Taiwan University (NTU), Taipei, Taiwan*
¹³⁵*Chulalongkorn University, Faculty of Science, Department of Physics, Bangkok, Thailand*
¹³⁶*Çukurova University, Physics Department, Science and Art Faculty, Adana, Turkey*
¹³⁷*Middle East Technical University, Physics Department, Ankara, Turkey*
¹³⁸*Bogazici University, Istanbul, Turkey*
¹³⁹*Istanbul Technical University, Istanbul, Turkey*
¹⁴⁰*Istanbul University, Istanbul, Turkey*
¹⁴¹*Institute for Scintillation Materials of National Academy of Science of Ukraine, Kharkov, Ukraine*
¹⁴²*National Scientific Center, Kharkov Institute of Physics and Technology, Kharkov, Ukraine*
¹⁴³*University of Bristol, Bristol, United Kingdom*
¹⁴⁴*Rutherford Appleton Laboratory, Didcot, United Kingdom*
¹⁴⁵*Imperial College, London, United Kingdom*
¹⁴⁶*Brunel University, Uxbridge, United Kingdom*
¹⁴⁷*Baylor University, Waco, Texas, USA*
¹⁴⁸*Catholic University of America, Washington, D.C., USA*
¹⁴⁹*The University of Alabama, Tuscaloosa, Alabama, USA*
¹⁵⁰*Boston University, Boston, Massachusetts, USA*
¹⁵¹*Brown University, Providence, Rhode Island, USA*
¹⁵²*University of California, Davis, Davis, California, USA*
¹⁵³*University of California, Los Angeles, California, USA*
¹⁵⁴*University of California, Riverside, Riverside, California, USA*
¹⁵⁵*University of California, San Diego, La Jolla, California, USA*
¹⁵⁶*University of California, Santa Barbara—Department of Physics, Santa Barbara, California, USA*
¹⁵⁷*California Institute of Technology, Pasadena, California, USA*
¹⁵⁸*Carnegie Mellon University, Pittsburgh, Pennsylvania, USA*
¹⁵⁹*University of Colorado Boulder, Boulder, Colorado, USA*
¹⁶⁰*Cornell University, Ithaca, New York, USA*
¹⁶¹*Fermi National Accelerator Laboratory, Batavia, Illinois, USA*
¹⁶²*University of Florida, Gainesville, Florida, USA*
¹⁶³*Florida State University, Tallahassee, Florida, USA*
¹⁶⁴*Florida Institute of Technology, Melbourne, Florida, USA*
¹⁶⁵*University of Illinois at Chicago (UIC), Chicago, Illinois, USA*
¹⁶⁶*The University of Iowa, Iowa City, Iowa, USA*
¹⁶⁷*Johns Hopkins University, Baltimore, Maryland, USA*
¹⁶⁸*The University of Kansas, Lawrence, Kansas, USA*
¹⁶⁹*Kansas State University, Manhattan, Kansas, USA*
¹⁷⁰*Lawrence Livermore National Laboratory, Livermore, California, USA*
¹⁷¹*University of Maryland, College Park, Maryland, USA*
¹⁷²*Massachusetts Institute of Technology, Cambridge, Massachusetts, USA*
¹⁷³*University of Minnesota, Minneapolis, Minnesota, USA*
¹⁷⁴*University of Mississippi, Oxford, Mississippi, USA*
¹⁷⁵*University of Nebraska-Lincoln, Lincoln, Nebraska, USA*
¹⁷⁶*State University of New York at Buffalo, Buffalo, New York, USA*
¹⁷⁷*Northeastern University, Boston, Massachusetts, USA*
¹⁷⁸*Northwestern University, Evanston, Illinois, USA*
¹⁷⁹*University of Notre Dame, Notre Dame, Indiana, USA*
¹⁸⁰*The Ohio State University, Columbus, Ohio, USA*
¹⁸¹*Princeton University, Princeton, New Jersey, USA*
¹⁸²*University of Puerto Rico, Mayaguez, Puerto Rico, USA*
¹⁸³*Purdue University, West Lafayette, Indiana, USA*
¹⁸⁴*Purdue University Northwest, Hammond, Indiana, USA*
¹⁸⁵*Rice University, Houston, Texas, USA*
¹⁸⁶*University of Rochester, Rochester, New York, USA*
¹⁸⁷*Rutgers, The State University of New Jersey, Piscataway, New Jersey, USA*
¹⁸⁸*University of Tennessee, Knoxville, Tennessee, USA*

¹⁸⁹*Texas A&M University, College Station, Texas, USA*

¹⁹⁰*Texas Tech University, Lubbock, Texas, USA*

¹⁹¹*Vanderbilt University, Nashville, Tennessee, USA*

¹⁹²*University of Virginia, Charlottesville, Virginia, USA*

¹⁹³*Wayne State University, Detroit, Michigan, USA*

¹⁹⁴*University of Wisconsin—Madison, Madison, Wisconsin, USA*

^aDeceased.

^bAlso at Vienna University of Technology, Vienna, Austria.

^cAlso at Institute of Basic and Applied Sciences, Faculty of Engineering, Arab Academy for Science, Technology and Maritime Transport, Alexandria, Egypt.

^dAlso at Université Libre de Bruxelles, Bruxelles, Belgium.

^eAlso at Universidade Estadual de Campinas, Campinas, Brazil.

^fAlso at Federal University of Rio Grande do Sul, Porto Alegre, Brazil.

^gAlso at University of Chinese Academy of Sciences.

^hAlso at Department of Physics, Tsinghua University, Beijing, China.

ⁱUniversidade Federal do Mato Grosso do Sul, Nova Andradina, Mato Grosso do Sul, Brazil [Universidade Federal do Mato Grosso do Sul = UFMS].

^jAlso at The University of Iowa, Iowa City, Iowa, USA.

^kAlso at Nanjing Normal University Department of Physics, Nanjing, China.

^lAlso at University of Chinese Academy of Sciences, Beijing, China.

^mAlso at Institute for Theoretical and Experimental Physics named by A.I. Alikhanov of NRC ‘Kurchatov Institute’, Moscow, Russia.

ⁿAlso at Joint Institute for Nuclear Research, Dubna, Russia.

^oAlso at Ain Shams University, Cairo, Egypt.

^pAlso at Zewail City of Science and Technology, Zewail, Egypt.

^qAlso at British University in Egypt, Cairo, Egypt.

^rAlso at Purdue University, West Lafayette, Indiana, USA.

^sAlso at Université de Haute Alsace, Mulhouse, France.

^tAlso at Erzincan Binali Yildirim University, Erzincan, Turkey.

^uAlso at CERN, European Organization for Nuclear Research, Geneva, Switzerland.

^vAlso at RWTH Aachen University, III. Physikalisches Institut A, Aachen, Germany.

^wAlso at University of Hamburg, Hamburg, Germany.

^xAlso at Department of Physics, Isfahan University of Technology, Isfahan, Iran.

^yAlso at Brandenburg University of Technology, Cottbus, Germany.

^zAlso at Skobeltsyn Institute of Nuclear Physics, Lomonosov Moscow State University, Moscow, Russia.

^{aa}Also at Physics Department, Faculty of Science, Assiut University.

^{bb}Also at Eszterhazy Karoly University, Karoly Robert Campus, Gyongyos, Hungary.

^{cc}Also at Institute of Physics, University of Debrecen, Debrecen, Hungary.

^{dd}Also at Institute of Nuclear Research ATOMKI, Debrecen, Hungary.

^{ee}Also at MTA-ELTE Lendület CMS Particle and Nuclear Physics Group, Eötvös Loránd University, Budapest, Hungary.

^{ff}Also at Wigner Research Centre for Physics, Budapest, Hungary.

^{gg}Also at IIT Bhubaneswar, Bhubaneswar, India.

^{hh}Also at Institute of Physics, Bhubaneswar, India.

ⁱⁱAlso at G.H.G. Khalsa College, Punjab, India.

^{jj}Also at Shoolini University, Solan, India.

^{kk}Also at University of Hyderabad, Hyderabad, India.

^{ll}Also at University of Visva-Bharati, Santiniketan, India.

^{mm}Also at Indian Institute of Technology (IIT), Mumbai, India.

ⁿⁿAlso at Deutsches Elektronen-Synchrotron, Hamburg, Germany.

^{oo}Also at Sharif University of Technology, Tehran, Iran.

^{pp}Also at Department of Physics, University of Science and Technology of Mazandaran, Behshahr, Iran.

^{qq}Also at INFN Sezione di Bari, Università di Bari, Politecnico di Bari, Bari, Italy.

^{rr}Also at Italian National Agency for New Technologies, Energy and Sustainable Economic Development.

^{ss}Also at Centro Siciliano di Fisica Nucleare e di Struttura Della Materia.

^{tt}Also at Università di Napoli ‘Federico II’, Napoli, Italy.

^{uu}Also at Riga Technical University, Riga, Latvia.

^{vv}Also at Consejo Nacional de Ciencia y Tecnología, Mexico City, Mexico.

^{ww}Also at IRFU, CEA, Université Paris-Saclay, Gif-sur-Yvette, France.

^{xx}Also at Institute for Nuclear Research, Moscow, Russia.

- ^{yy} Also at National Research Nuclear University 'Moscow Engineering Physics Institute' (MEPhI), Moscow, Russia.
- ^{zz} Also at St. Petersburg State Polytechnical University, St. Petersburg, Russia.
- ^{aaa} Also at University of Florida, Gainesville, Florida, USA.
- ^{bbb} Also at Imperial College, London, United Kingdom.
- ^{ccc} Also at P.N. Lebedev Physical Institute, Moscow, Russia.
- ^{ddd} Also at Moscow Institute of Physics and Technology, Moscow, Russia.
- ^{eee} Also at California Institute of Technology, Pasadena, California, USA.
- ^{fff} Also at Budker Institute of Nuclear Physics, Novosibirsk, Russia.
- ^{ggg} Also at Faculty of Physics, University of Belgrade, Belgrade, Serbia.
- ^{hhh} Also at Trincomalee Campus, Eastern University, Sri Lanka.
- ⁱⁱⁱ Also at INFN Sezione di Pavia, Università di Pavia, Pavia, Italy.
- ^{jjj} Also at National and Kapodistrian University of Athens, Athens, Greece.
- ^{kkk} Also at Universität Zürich, Zurich, Switzerland.
- ^{lll} Also at Ecole Polytechnique Fédérale Lausanne, Lausanne, Switzerland.
- ^{mmm} Also at Stefan Meyer Institute for Subatomic Physics, Vienna, Austria.
- ⁿⁿⁿ Also at Laboratoire d'Annecy-le-Vieux de Physique des Particules, IN2P3-CNRS, Annecy-le-Vieux, France.
- ^{ooo} Also at Gaziosmanpasa University, Tokat, Turkey.
- ^{ppp} Also at Şırnak University, Şırnak, Turkey.
- ^{qqq} Also at Near East University, Research Center of Experimental Health Science, Nicosia, Turkey.
- ^{rrr} Also at Konya Technical University.
- ^{sss} Also at Istanbul University—Cerraphasa, Faculty of Engineering.
- ^{ttt} Also at Mersin University, Mersin, Turkey.
- ^{uuu} Also at Piri Reis University, Istanbul, Turkey.
- ^{vvv} Also at Adiyaman University, Adiyaman, Turkey.
- ^{www} Also at Tarsus University, Tarsus, Turkey.
- ^{xxx} Also at Ozyegin University, Istanbul, Turkey.
- ^{yyy} Also at Izmir Institute of Technology, Izmir, Turkey.
- ^{zzz} Also at Necmettin Erbakan University, Konya, Turkey.
- ^{aaaa} Also at Bozok Universitetesi Rektörlüğü, Yozgat, Turkey.
- ^{bbbb} Also at Marmara University, Istanbul, Turkey.
- ^{cccc} Also at Milli Savunma University, Istanbul, Turkey.
- ^{dddd} Also at Kafkas University, Kars, Turkey.
- ^{eeee} Also at Istanbul Bilgi University, Istanbul, Turkey.
- ^{fff} Also at Hacettepe University, Ankara, Turkey.
- ^{gggg} Also at Vrije Universiteit Brussel, Brussel, Belgium.
- ^{hhhh} Also at School of Physics and Astronomy, University of Southampton, Southampton, United Kingdom.
- ⁱⁱⁱⁱ Also at IPPP Durham University, Durham, United Kingdom.
- ^{jjjj} Also at Monash University, Faculty of Science, Clayton, Australia.
- ^{kkkk} Also at Bethel University, St. Paul, Minneapolis, USA.
- ^{llll} Also at Karamanoğlu Mehmetbey University, Karaman, Turkey.
- ^{mmmm} Also at Bingol University, Bingol, Turkey.
- ⁿⁿⁿⁿ Also at Georgian Technical University, Tbilisi, Georgia.
- ^{oooo} Also at Sinop University, Sinop, Turkey.
- ^{pppp} Also at Mimar Sinan University, Istanbul, Istanbul, Turkey.
- ^{qqqq} Also at Erciyes University, Kayseri, Turkey.
- ^{rrrr} Also at Texas A&M University at Qatar, Doha, Qatar.
- ^{ssss} Also at Kyungpook National University, Daegu, Korea.